AD616904

January 31, 1962

*Final Report*

# RESEARCH ON COLLISION PROCESSES OF ELECTRONS AND ATOMS

*Prepared for:*

OFFICE OF NAVAL RESEARCH
DEPARTMENT OF THE NAVY BLDG. T-3
WASHINGTON 25, D.C.

CONTRACT Nonr-2588(00)

*By:* James R. Peterson Charles J. Cook

*SRI Project No. SU-2557*

*Approved:*

Clinton M. Kelley

CLINTON M. KELLEY, DIRECTOR
DIVISION OF CHEMICAL PHYSICS



Copy No. 5

## ABSTRACT

A description is given of the apparatus and method used in the measurement of cross sections for the ionization of atoms and molecules by electron impact. A cross-beam technique is employed, using a beam of fast atoms of 2 to 3 kev kinetic energy as a target. Product ions are analyzed according to their charge/momentum. Sources of spurious ion currents and other interference are discussed. Absolute cross sections were measured for incident electron energies ranging from below threshold to 500 ev; results are presented and discussed for the ionization of nitrogen and argon atoms, and for nitrogen molecules. The cross section for $e + N \rightarrow N^+ + 2e$ has an energy dependence rather similar to the theory of Seaton, but is about 20% smaller. The dissociative ionization cross section for $N_2$ does not appear to be a direct process (i.e., occurring in less than $10^{-7}$ sec) for electron impact energies below 50 ev.

# CONTENTS

# ILLUSTRATIONS

# I INTRODUCTION

This report summarizes the research carried out under Office of Naval Research Contract Nonr-2588(00),* with special emphasis on the work during the period 1 October, 1960 to 31 January, 1962. This experimental research program has been directed toward measuring the interaction cross sections for the ionization of nitrogen and oxygen atoms by electron impact.

* Funded by the Advanced Research Projects Agency, ARPA Order 5-58 Task Order 2.

## II RESUMÉ OF THE PROGRAM

An experimental investigation of electron-atom interactions, such as $e + N \rightarrow N^+ + 2e$, is inherently difficult because of the problem of obtaining free atoms, which exist stably only in the molecular state. Consequently, a volume containing free atoms generally will be contaminated by a far greater density of other molecules. There results not only the problem of obtaining reactant atoms in sufficient numbers to measure the reaction products, but also the task of distinguishing between the desired reactions and the large number of other reactions that occur in the interaction volume.

Our approach to the problem has been described in the first Annual Report[1] and will be summarized here. The instability of free atoms limits feasible methods to those involving crossed beams of electrons and atoms: we have chosen a novel variation of this technique which utilizes a fast ion beam as a source of the atom beam. A schematic diagram of the apparatus is shown in Fig. 1.

A fairly intense beam of atomic and molecular ions is extracted from an rf ion source[2] at an arbitrary energy in the range 2-5 kev. The beam is focused and sent through a wedge-shaped magnetic field which deflects the atomic ions through 90° and seperates them from the molecular ions. The emerging atomic ion beam is then refocused and passes through a "charge transfer" cell containing a gas at a relatively high pressure, about $7 \times 10^{-4}$ torr. About 10% of the ions undergo charge-transfer collisions in traversing this region, and become neutral atoms without experiencing any significant change in momentum. The remaining ions are then deflected by an electrostatic field and the remaining beam of neutral atoms enters a magnetic field where it is intersected by an electron beam. Ions created from the fast beam atoms by electron collisions in this region retain their original momentum and are deflected by the magnetic field and focused to a collector, while the neutral-beam atoms pass on through and are stopped by a thin-film thermocouple which

serves as a neutral beam monitor. The neutral beam is sufficiently energetic that its density may be ascertained from a measurement of the temperature rise in the thin nickel film which stops the beam.

The electron beam is square-wave modulated; the ion current is amplified by a tuned amplifier and measured by a synchronous detector. The kinetic energy of the beam electrons is adjustable so that ion currents may be measured as a function of electron energy.

During the course of the program, the apparatus, shown in Fig. 2, has been built and has undergone many refining modifications. Not too surprisingly, a rather large number of complex problems were discovered during the preliminary investigations of the behavior of the apparatus, and considerable effort was given to understanding and surmounting the obstacles. In August 1961 the long preliminary work culminated in the first useful measurements obtained—the cross section for the ionization of nitrogen atoms. Since then, further refinements in both the equipment and the measuring technique have been made, along with more detailed studies of some of the problems.

The initial measurements of atomic nitrogen beams, were followed up by studies of molecular nitrogen and argon beams. In the following discussions we shall refer to the processes and their interaction cross sections as follows:

| BEAM | REACTION | CROSS SECTION |
|---|---|---|
| N | $e + N \rightarrow N^+ + 2e$ | $Q(N^+)$ |
| $N_2$ | $e + N_2 \rightarrow N_2^+ + 2e$ | $Q(N_2^+)$ |
| $N_2$ | $e + N_2 \rightarrow N + N^+ + 2e$ | $Q(N_2^+ \text{ diss})$ |
| $N_2$ | $e + N_2 \rightarrow N_2^{++} + 3e$ | $Q(N_2^{++})$ |
| Ar | $e + Ar \rightarrow Ar^+ + 2e$ | $Q(Ar^+)$ |
| Ar | $e + Ar \rightarrow Ar^{++} + 3e$ | $Q(Ar^{++})$ |

## III DETAILS OF THE METHOD AND DISCUSSION OF THE MEASUREMENTS

### A. DETAILS OF THE METHOD: ADVANTAGES AND PROBLEMS

There are several important advantages to the method, as well as some problems connected with it. The advantages it has over the conventional, thermal atomic beam method are: (1) Complete separation of the target atoms from the parent molecules—effected by the mass analysis of the ion beam—allows studies to be made on many different atoms and molecules which would not be possible with a thermal beam. (2) The target atoms are distinguished by their unique momentum, which allows the mass analysis of product ions and eliminates some secondary reactions—only those ions having the proper momentum (of the incident neutral beam) are focused to the collector, and the large number of ionized ambient gas molecules formed in the electron beam path are not collected. (3) The method permits the direct measurement of absolute cross sections; hence, measurements need not be made relative to some previously measured cross section.

The main problems are caused by low signal levels, due to low beam densities, and by extraneous, interfering reactions, due to background gas-beam interactions that compete with the one under study. Low beam densities result from space-charge limitations of the ion beam and also from difficulties in maintaining the beam density over the distances involved, particularly between the final focusing lens (in front of the change-transfer cell) and the beam intersection region. The neutral beam densities are low, but not prohibitively so. Low signal levels are an inherent characteristic of all crossed-beam measurements; only recently have detection techniques become sufficiently refined to permit the crossed-beam method to be successfully employed.[3]

There are certain types of interference that are peculiar to our method. The fast beam atoms have sufficient energy to ionize and excite the ambient gas along the beam path, and to undergo charge-loss collisions, etc. These reactions can yield a high level of background current at the ion collector, which raises the noise level in the detector but does not directly interfere with the modulated signal. However these steady-state currents, by their interaction with the modulated space charge potential

of the electron beam, can produce spurious signals. Spurious signals can also arise from interaction of the fast atoms with a modulated component of the gas in the interaction region produced by the electron beam. These and other types of interferrence have been discussed in the Annual and Quarterly Reports issued under the contract, but because of their significant influence on the course of this program, we will review them below.

There are three variable quantities that enter into the cross-section computations, as well as several constant factors. The measured variables are the electron beam current, i.e., the current which crosses the interaction region; the voltage output, $V_g$, of the neutral beam detector which determines the atom beam current; and the signal, $d$, from the phase-sensitive detector which measures the product ion current delivered to the collector. The ion beam energy, the geometrical factors, and the detector sensitivities remain essentially constant from run to run.

The details of the method will be presented in the following order: we shall describe (1) the apparatus and instruments used in the measurement of the three variables, and then (2) the behavior of these variables, especially the observed ion signal, under different tests. We will then discuss the operating procedures, some of which were necessitated by the results of the tests.

## 1. Measurement of Various Currents and Parameters

The system of signal detection and measurement was described in the Second Annual Report.[4] A block diagram of the arrangement of components is given in Fig. 3. The currents of the electron beam, atom beam, and product ions were measured as follows:

### a. Electron Beam

Currents to various elements of the electron gun, shown schematically in Fig. 4, are measured by conventional, 100 $\mu$a full scale, dc meters with suitable shunts to allow currents of 10 ma to be measured. The potentials of the elements are measured with a vacuum tube voltmeter, which is periodically calibrated against accurately known reference voltages obtained from a Keithley Model 241 Regulated High Voltage supply.

### b. NEUTRAL BEAM

The neutral beam detector, shown in Fig. 5, was described and analyzed in the Second Annual Report.[4] (A report on this detector is being written for publication.) The beam is stopped by a thin ($10^{-4}$ cm) nickel film, to the back side of which is soldered a $10^{-4}$ inch-diameter Nichrome wire to form a thermocouple. The beam dissipates its power in the nickel film, and the consequent temperature rise leads to a change in the output voltage of the thermocouple, which is measured by a Keithley Model 150-A microvoltmeter-ammeter.

The sensitivity of the detector is determined with an ion beam (no gas in the charge-transfer cell), by successive measurements of the thermocouple output voltage and the total ion current with secondary electrons suppressed. These checks are made fairly frequently and individual measurements seldom vary by more than 5%. Recently, however, rather severe (~20%) fluctuations were noticed in the detector output during cross-section measurements, and the ion current signal remained relatively constant. The effect was thought at first to be due to severe inhomogeneities in the atom beam which could change position on the thin film with small changes in the beam energy. The thermocouple ultimately ceased functioning, and when the interaction chamber was opened up, it was found that the beam had eroded (sputtered) a small ¼-inch-diameter hole out of the film, centered at the thermocouple so that the Nichrome wire was left dangling in space. The fluctuations in sensitivity doubtlessly occurred when this hole was being formed. To avoid this problem in the future, the thin films will be replaced frequently. At a beam energy of about 2850 ev the present detector yields an output voltage change of about 0.110 millivolt per microamp of beam current, or about 38.5 microvolts per milliwatt.

### c. PRODUCT ION CURRENT

The total ion current reaching the collector consists of an 89 cps square-wave modulated current superimposed on a constant background current. This background current, caused by electron loss collisions with ambient gas molecules in and near the beam interaction volume, exceeds the wanted signal by about two orders of magnitude. The voltage developed by the total current as it flows through a $10^9$ ohm resistance, appears on the grid of the first tube (located inside the

vacuum system) of the unit-gain preamplifier, shown in Fig. 6, whose output impedance is relatively low ($10^6$ ohms). The main amplifier (Fig. 7) boosts the signal to a level which is easily detected and measured. In order to avoid saturation by noise, the amplifier is tuned to amplify only those frequencies lying within a narrow pass band centered at the modulation frequency. The phase-sensitive detector (Fig. 7) rectifies the output of the amplifier in phase with a reference signal, and the resulting dc voltage is plotted by one channel of a two-pen strip-chart recorder. (The other channel records the output of the neutral beam monitor.) The effective bandwidth of the system can be reduced below that of the main amplifier by increasing the time constant at the output of the detector. Such a reduction of the bandwidth has the effect of increasing the signal-to-noise ratio. We have placed an R-C net of variable time constant in the detector output for this purpose.

The electron beam modulator and the phase-sensitive detector are both controlled by a single oscillator (Fig. 8) through appropriate phase-shifting networks. The relative phases of the electron beam modulation pulse and the detector reference signal are observed simultaneously on a Hewlett-Packard Model 122-A dual channel oscilloscope. The difference $\Delta\phi$ between the phase of the reference signal and the modulation pulse is recorded and may be changed by either phase-shifting network.

The preamplifier circuit is shown in Fig. 6. It consists of two CK512AX tubes in cascade with another CK512AX as cathode-follower output, also providing the 100% negative feedback signal. The open-loop gain (without feedback) is about 33. The closed-loop gain (with feedback) was not measured because there is no simple way to introduce a known signal to the high-impedance grid without destroying the effective feedback. An analysis of the circuit showed that a net gain of 0.97 results from an open-loop gain of 33, for a measured input circuit capacitance of $7 \times 10^{-12}$ farad and a grid-cathode capacitance of $2 \times 10^{-12}$ farad. The CK512AX tubes are not very sturdy; they require frequent checks and must be replaced frequently to keep the circuit noise level to a minimum. New tubes are checked for their grid and plate current characteristics before they are used, and are rejected if found unsatisfactory.

The amplifier, shown schematically in Fig. 7, has been modified since it was last described in the second Annual Report.[4] The noise level was reduced and the stability increased, but the bandpass and gain

characteristics have not been changed significantly. The three filters, which provide a bandwidth of about one cycle per second, are tuned to the 89 cps signal from the oscillator. Since the phase shift through the tuned amplifier is highly frequency-dependent, the oscillator must be exceedingly stable. A change in frequency of 0.1 cps results in a 20° change in the phase shift through the amplifier. Even though the gain of the amplifier is relatively unchanged during this small shift, the phase-sensitive detector receives a signal which is 20° from the correct value, and the output is reduced by 6% (1 - cos 20°). One other interesting characteristic of the amplifier is that the phase shift produced is dependent on the magnitude of the signal. This effect is probably due to a partial saturation of the filter inductances which have a very high $Q$ for small currents but show saturation effects very easily. Figure 9 shows a typical relationship between the output signal $d$ and $\Delta\phi_{100} - \Delta\phi_d$, the difference between the phase shift at full scale output (100 divisions on the reccrder) and an arbitrary output in signal level $d$. During the actual runs, the phase of the reference signal was set for the optimum value for the observed signal strength according to this relationship.

The phase-sensitive (synchronous) detector, shown in Fig. 7, is unchanged from that shown in the second Annual Report.

The sensitivity of the amplifier and detector is determined by feeding the known signal from the calibrator (shown in Fig. 7) into the amplifier. The amplifier gain is usually set so that the over-all sensitivity of the amplifier-detector is such that a recorder reading of 91 divisions is produced by a sinusoidal input signal of 100 microvolts peak-to-peak. At this sensitivity, the recorder reads full scale (100 divisions) for an ion current of $8.6 \times 10^{-14}$ amp during the "on" portion of the modulation period.

The original oscillator produced small frequency drifts with fluctuations in line voltage, room temperature, drafts of air, etc., and thus produced changes in the phase shift in the amplifier. Consequently, this oscillator was replaced by a very stable tuned-fork oscillator, and the modulator and phase shifting network were added, as shown in Fig. 8. The basic oscillator is tuned to 712 cps, and this is followed by binary dividers so that outputs of 712, 356, and 89 cps are provided. The 89 cycle signal is used for the present work, and is so stable that no phase shift variations are noticeable over time intervals of several days.

## 2. Characteristics of the Observed Quantities and Description of the Interfering Processes

It has been mentioned that interference is observed under a variety of conditions. In discussing the behavior of the observed signal when different parameters on the machine are varied, it is possible to indicate many types of interference, and to point out the major sources of difficulty in the experiment.

### a. Dependence of Observed Signals on Electron Gun Conditions

A signal at the ion detector was observed when only the electron beam was on and there was no intersecting atom beam. A study was made of this signal with variations of the magnetic field, electron energy, and bias voltages placed between grids $G_2$, $G_3$ and the collector $A$ of the gun (see Fig. 4). Usually the phase of the signal was recorded, in addition to its amplitude, in an attempt to gain some insight of the nature of the source or sources of these extraneous currents. This signal was found to depend on the strength of the magnetic field present in the region of the electron beam and on the direction of the field as well, which is astonishing since the fields were all too strong to permit any charged particles (at the low kinetic energies possible in this case) from traveling directly from the beam region to the collector. The signal also depended on the electron beam energy; the graph of signal *vs* beam energy shows an apparent threshold at about 20 ev; the curve then rises to a maximum of about 70 ev and falls off quickly again to about $^1/_7$ the peak value at about 120 ev; then gradually decreases at higher energies. Some structure appears on the low energy side of the peak, but no detailed studies of this feature have been made. To increase the complexity, the signals change in magnitude when the polarity of the voltage on a secondary particle suppressor (located in front on the collector) is changed, as might be expected, but the *polarity* of the signal is unchanged, its phase changes by only 10°, from a lag of about 85° to one of about 75° when the suppressor voltage is changed from −45 to +45 v. Thus there are at least two, and probably more, sources of these anomalous currents. The seriousness of the problem was essentially eliminated when it was discovered that all of these signals which are due to the electron beam can be eliminated by placing a small electric field across the drift space in the electron gun. As may be seen in Fig. 10, when a voltage difference $V_3 - V_2 = 2.5$ ev is placed between

grids $G_2$ and $G_3$, signals from the gun alone are undetectable. It has been concluded that charged particles in the drift space are intimately connected with the spurious signals, but further explanations are only speculative.

The above discussion describes the signals due only to the electron beam. They are sufficiently strong to mask the ion currents sought after in the actual experiments, but are easily eliminated by a bias across the drift space. However it was found that even with the weak electric field present between the drift grids, spurious currents were observed when the atom beam was present and intersecting the electron beam under the intended conditions of measurement. The effect of these currents was to yield a computed ionization cross section at least an order of magnitude larger than anticipated, and which did not have a physically realistic behavior at low electron energies: The apparent "cross section" for $e + N \rightarrow N^+ + 2e$ had a maximum at about 100 ev and, as the electron beam energy was reduced, the cross section decreased to a minimum at about 25 ev and then INCREASED at energies below the actual threshold of 14.5 ev. (This effect was described in Quarterly Letter Report No. 7.) A study of the behavior of the signal under the variation of several parameters was made and it was found that the spurious component could be eliminated by the application of an electric field between the second drift grid $G_3$ and the collector $A$. Figure 11 shows the relationship between the signal and the bias voltage $V_A - V_2$, with $V_3 - V_2 = 2.5$ ev, for 70-ev electrons. As $V_A - V_2$ was increased from 0 to about 22 v, the signal decreased monotonically until it reached a plateau of $\frac{1}{4}$th the original value. On this plateau, at $V_A - V_2 > 15$ v, the signal was independent of $V_3 - V_2$, as well as $V_A - V_2$. The actual cross-section measurements were made with $V_3 - V_2 = 2.5$ v, and $V_A - V_2 = 17.5$ v or higher.

Under these conditions the observed signal due to the ionization of incident beam atoms by electron impact was independent of any gun bias, and had a realistic dependence on electron energy near the ionization threshold.

In summary, spurious signals dependent on both the electron and atom beams are eliminated by a suitable electrostatic field between the second drift grid and the electron collector. Thus they seem to be related ultimately to some charged species created at or near the electron

collector which interacts either primarily or secondarily with the atom beam. Since no significant phase lag was observed, the events leading to these signals are prompt compared to $10^{-7}$ sec.

### 6. DEPENDENCE OF THE SIGNAL FROM CROSSED BEAMS ON THE VALUE OF THE MAGNETIC FIELD

When the observed signals (with the optimum biases on the electron gun) were plotted against the magnetic field surrounding the gun, the resulting curve was more complicated than expected. In the case of the atoms, the desired $N^+$ peak occurred at about 3.2 kgauss, but a very strong signal was also observed at about 1.9 kgauss, and these two peaks were separated by a region where the signal was negative. An examination of the behavior of the anomalous 1.9 kgauss signal, which was many times stronger than the $N^+$ signal over all electron energies, led to the conclusion that it was due in some way to the small ionized component of the incident neutral beam. These ions are created from beam atoms by electron-loss collisions with ambient gas molecules in the beam path between the ion deflector plates and the beam-intersection region. A second set of deflector plates was installed just a short distance in front of the magnet to eliminate ions formed after the beam had passed through the first deflector but before it entered the second. A marked reduction in the anomalous positive and negative peaks resulted.

Although only an exceedingly small fraction of the neutral beam particles become ionized after passing through the first deflectors, the charged current so developed may be orders of magnitude larger than that resulting from the electron interactions in the intersection region, which is smaller than the effective current of the neutral beam by a factor of at least $10^7$. These "incident" ions begin their curved paths immediately as they enter the magnetic field, and will therefore reach the ion collector at considerably lower field strengths than those formed in the intersection region. They are unmodulated by the electron beam except possibly by its space charge. The weak electrical fields associated with the space charge potential will cause a slight alteration of the trajectories of the incident ions which pass through part of the intersection region. If the incident ions form a diffuse "beam" which is only partially collected, as is likely, the action of the space charge fields can cause either a greater or a smaller ion current to reach the collector: the number of incident ions reaching the collector can be modulated to cause either a positive or a negative signal. The second deflector reduced the

anomalous peak by an order of magnitude; however, there was still a residual signal which was probably due to ions formed in the short path length between the second deflector and the gun. It is important to note that the observed anomalous signal is much smaller than would be observed if the entire incident ion current developed in 1 cm of path length were 100% modulated; therefore, the electron beam need only cause a minor modulation of this steady state beam.

We have also observed the dependence of the detected signal on the magnetic field in the cases of $N_2$ and Ar neutral beams. Each of the curves had anomalous peaks which were incompatible with the properties of signals due to the desired electron-neutral beam interactions: The ratio $d/V_t$ of the signal to the neutral beam detector output depended upon the neutral beam current (or perhaps on the ambient gas density in the beam path, which increased with the beam). It also had a nonlinear dependence on the electron beam current. Finally, it depended on the polarity of the ungrounded side of the second deflector. This deflector was arranged so that one of the plates was always grounded while the other could be made either positive or negative. The anomalous signals were much smaller when the deflector potential was negative than when it was positive. Figure 12 shows the variation of the signal (normalized to the neutral beam intensity) with magnetic field, when the deflector voltage was *positive*. Several combinations of neutral beam intensities ($V_t$) and electron beam currents ($i_e$) and energies ($V_e$) are represented. At an electron energy of 100 ev, two real product ion peaks are seen. The 3.2 kgauss peak corresponds to the $N_2^+$ ions and the 1.6 kgauss peak is due to $N_2^{++}$ and $N^+$ (dissociative ionization of $N_2$). The anomalous peak at 2.2 kgauss is presumably due to "incident" $N_2^+$ ions; it has the same position relative to the real $N_2^+$ peak as the anomalous incident $N^+$ peak did to that formed by product $N^+$ ions in the atomic case. The peak at 1.1 kgauss is possibly due to either incident $N_2^{++}$ or $N^+$ (dissociated) ions, although this point is not clear. This peak was almost absent when the deflector polarity was reversed. Note the negative dips adjoining the positive anomalous peaks.

The curve in Fig. 13 represents the normalized signal ($d/V_t$) from an argon beam at 100 ev electron energy, when the second deflector potential was *negative*. The $A^+$ and $A^{++}$ peaks are easily seen, and a small anomalous peak due to incident $A^+$ ions is indicated. The curve actually goes slightly negative to the right of this peak.

The actual cross section measurements were made with a negative potential on the second deflector.

## B. PREMEASUREMENT CHECKS AND PROCEDURES

Each measurement was preceded by a number of checks made on the apparatus to make certain that the apparatus was functioning properly and that the many operating parameters were set in accordance with the conclusions reached from the above mentioned studies of interference. These procedures may be grouped according to whether they pertained to the ion accelerator and neutral beam apparatus or to the components of the interaction chamber and detection apparatus.

### 1. Ion Source and Neutral Beam Checks

#### a. ESTABLISHING THE ION BEAM

The gas flow to source, rf power, focusing voltages, and analyzing magnet current were adjusted to obtain maximum ion beam (ion deflectors off) to the neutral detector in the interaction chamber. These parameters were optimized for maximum beam with minimum current fluctuations to reduce beam noise. Beam current fluctuations were generally due to arcing in the beam extraction region of the source. These adjustments were made with the neutral detector operating as a Faraday cup with secondary electron suppression, and using the Keithley 15GA as a microammeter.

#### b. NEUTRAL DETECTOR SENSITIVITY

With the ion beam maximized, a series of runs were made in which the neutral detector was used alternately to measure the ion beam current and then the output of the thermocouple. $V_t/i_a/E_a$, the ratio of the thermocouple output to the beam current, divided by the beam energy, was used as the neutral detector sensitivity in the cross-section calculations. The measured sensitivity was usually about 39 microvolts per milliwatt, or $3.9 \times 10^{-2}$ v/w.

#### c. ESTABLISHING THE NEUTRAL ATOM BEAM

After calibrating the neutral detector with the ion beam maximized at the detector, the ion deflectors were turned on, the neutral

detector was set to measure the thermocouple output, and gas was admitted to the charge-transfer cell. The flow was set to yield a neutral beam optimized against the rising gas pressure in the interaction chamber. These pressures ranged from about $1 \times 10^{-7}$ to $3 \times 10^{-7}$ torr. Minor changes in the voltages on the ion beam focusing lens, ahead of the charge-transfer cell, were sometimes made at this point in order to maximize the neutral beam.

### 2. Equipment Checks Pertaining to the Interaction Chamber

#### a. Checks Made on the Electron Gun

These consisted only of properly setting the various voltages on the drift grids and collector to eliminate the background signals.

#### b. Calibration of the Amplifier and Detector

After the installation of the tuned fork oscillator, the stability of the signal was such that the amplifier tuning required checking only every few days. Before each run, however, the reference signal was checked for proper amplitude, and the phase shift through the amplifier and the amplifier gain was measured for a known input signal. If any deviations from the normal values were found, proper adjustments were made. The operation of the preamplifier was checked by placing a calibrating signal on the guard electrode (electron suppressor) located in front of the ion collector. The capacitance between this electrode and the collector (about $8 \times 10^{-12}$ farad) was used to carry the signal to the preamp. This is the only method of checking the preamp when the system is under vacuum, since the first stage of the circuit is located inside the vacuum chamber and direct coupling cannot be achieved. The detector output for a given input was compared with similar measurements taken when the open-loop gain of the preamplifier could be checked directly.

#### c. Optimizing the Interaction Chamber Magnet Current and the Phase of the Detector

These parameters were finally adjusted from their predetermined approximate values by maximizing a signal which was known to correspond to a relatively large cross section and which was free from interference. The optimum phase angle was very reproducible from day to day, taking into account the variation with signal level shown in Fig. 9. The magnet setting was also constant for a given ion beam energy.

## C. CALCULATION OF THE CROSS SECTIONS

Consider an atom beam of uniform-volume density $\rho_a$ atoms/cm$^3$ confined to a rectangular cross-sectional area of lateral dimension $S$ cm and height $H$ cm, which is intersected perpendicularly, as shown schematically in Fig. 14, by an electron beam of uniform current density $j_e$ amp/cm$^2$, dimension $L$ cm in the direction of the atom beam, and height $H$ cm. The volume in which the two beams interact is $LSH$ cm$^3$. If the cross section for interaction is $Q$ cm$^2$ per atom, the number of ions produced per second, $dN^+/dt$, can be expressed as

$$\frac{dN^+}{dt} = \frac{\rho_a j_e SLHQ}{e}$$

where $e$ = absolute value of the electron charge (coulomb). If each ionized atom carries a charge $q$, and all of these ions are collected, the resulting current is

$$i^+ = q\frac{dN^+}{dt} = \left(\frac{q}{e}\right)\rho_a j_e SLHQ \text{ amp} \quad ,$$

and the cross section is given by

$$Q = \frac{e}{q}\frac{i^+}{\rho_a j_e SHL} \text{ cm}^2 \quad . \tag{1}$$

Experimentally, we do not measure $\rho_a$, $j_e$, and $i^+$ directly but determine them from the neutral detector output voltage $V_t$, the average electron gun current $i_e/2$, and the deflection $d$ of the recorder at the output of the ion current detector.

We obtain $j_e$ by measuring the total electron current $i_e$ flowing to the second drift grid $G_3$ and the collector $A$ (thus the current which crosses the drift space). The cross-sectional dimensions of the electron beam are assumed to be $L \times H$, those of the aperture in the control grid $G_1$ which is the smallest aperture in the electron beam path. Thus, we have an (average) current density

$$j_e = \frac{i_e}{LH} \quad . \tag{2}$$

Since we measure the electron current on a dc meter, we actually read $i_e/2$, the average over a complete cycle.

The atom volume-density $\rho_a$ is obtained from the atom beam energy $E_a$ (electron volts) and the thermocouple output voltage $V_t$ (volts), as follows: We measure the total atom beam current $i_a$ (expressed in amperes equivalent) which passes through the rectangular atom-beam defining aperture of dimensions $S \times H$ cm; thus the atom beam current density is $j_a = i_a/SH$ amp/cm$^2$. This current is measured in terms of its power, $i_a E_a$ watts, delivered to the neutral beam detector, whose sensitivity $z$ is determined with a pure ion beam and is given by

$$z = \frac{V_t}{i_a E_a} \text{ volts/watt} \quad .$$

Thus

$$i_a = \frac{V_t}{zE_a} \text{ amp} \quad ,$$

and

$$j_a = \frac{V_t}{zE_a SH} \text{ amp/cm}^2 \quad . \tag{3}$$

Finally, the volume density $\rho_a$ of a beam of particles of mass $M$ (amu), kinetic energy $E_A$ (ev), and current density $j_a$ (amp/cm$^2$) is given by

$$\rho_a = 4.4 \times 10^{12} \, j_a \left(\frac{M}{E_a}\right)^{1/2} \text{ atoms/cm}^3 \quad . \tag{4}$$

Combining (3) and (4), we find that a neutral detector output of $V_t$ volts indicates an atom volume density of

$$\rho_a = 4.4 \times 10^{12} \, \frac{V_t}{zSH} \left(\frac{M}{E_a^3}\right)^{1/2} \text{ atoms/cm}^2 \quad . \tag{5}$$

The ion current $i^+$ is computed from the output of the amplifier and synchronous detector as follows. The net gain of the preamplifier was calculated to be 0.97. The sensitivity of the tuned amplifier and detector is preset so that the recorder output $d$ is 91 divisions per 100 microvolts input (peak-to-peak sine wave) to the amplifier. If an

ion current of $i^+$ amp is modulated to form a square wave across the preamp input resistance of $10^9$ ohms, the recorder output deflection will be $d = 1.12 \times 10^{15}\ i^+$ divisions, whence

$$i^+ = 8.9 \times 10^{-16}\ d \text{ amperes} \qquad (6)$$

during the half-period that the ions are being collected.

## D. MEASUREMENT PROCEDURES: "SUBTRACTION" AND "SLOPE" METHODS

The data were taken in one of two ways, or by a combination of the two. The original data reported in the last Quarterly Report were taken in a series of runs during which the electron beam current remained at about the same value. The modulation voltage was set at each energy point to cut off the electron beam completely during half the modulation cycle; therefore, the average electron current read on the dc meters was just half of the current responsible for the ion signal observed. During these early runs the square wave modulation voltage was centered about the cathode potential, so that the electron beam density was a function of only the modulation voltage amplitude and the beam energy in the drift space. Because the ion signal observed with the atom beam *off* seemed to change somewhat with the gun conditions, these runs were made by alternately observing the signal with the atom beam on and off. The difference in the signal levels was taken for each "on" - "off" pair, and was considered to be due to the atom beam only. In this way any variation in the background due to the electron beam alone was subtracted out. Occasional checks were made to ascertain that there was a linear dependence of the signal on the electron beam current, but this was not done for each run. We shall call this the "subtraction" method. The neutral beam was monitored constantly and its intensity was averaged over each run for use in calculating the cross sections.

Recent measurements were made after the gun had been modified to allow a variable dc bias to be placed on the control grid $G_1$, so that the electron current could be adjusted to any energy without changing the modulation square wave amplitude. This allowed the current to be reduced to low values even at high electron energies with assurance that the current was still being cut off completely during half the modulation cycle. Accordingly, a "slope" method could easily be used: At a constant

electron energy, the ratio of signal to neutral beam monitor output, $i^+/V_t$ is plotted against $i_e$, and the slope, $\Delta i^+/(\Delta i_e V_t)$, of the straight line best fitting the points is used as the value of $i^+/i_e V_t$ in calculating the cross sections. This method is comparatively fast and has the virtue of providing a check on the linearity of the signal with $i_e$, but it does not allow for the effect of any changing background signal due to the gun alone.

In some measurements the two methods were combined. This is undoubtedly the safest procedure; however, it more than doubles the time required to take the data. On the other hand, occasional cross checks made using either the subtraction or the slope method have warranted their continued use during these essentially exploratory measurements.

# IV RESULTS

The experimental results are shown in Figs. 15, 16, and 17. The errors and uncertainties associated with these results are discussed in the following sections.

## A. ATOMIC NITROGEN

The data for $e + N \rightarrow N^+ + 2e$ are presented in Fig. 15. The curves are approximate fits to both the original data taken by the subtraction method and the more recent data obtained from the slope method. The curve has only been drawn for energies below 200 ev, where enough points were taken to provide a satisfactory average. The scatter of points indicates that the data are reproducible to about 10%. The absolute accuracy is less well known. Although there is a concurrent program to measure $Q(N^+)$ using a thermal beam,[5] no other experimental determinations have been made on N which can be referred to for comparison. However, the theoretical results of Seaton[6] are plotted along with our data in Fig. 15. The maximum cross section occurs at about 100 ev for each curve; however, below 200 ev our results are about 30% lower than those of Seaton. The two single points taken at 300 and 500 ev will be remeasured.

## B. MOLECULAR NITROGEN

These data are shown in Fig. 16. The total ionization cross section for $N_2$ as determined by Tate and Smith[7] is also shown in Fig. 16. The subtraction method data were taken on the $N_2^+$ peak only. The slope method was used to determine the cross sections for production of ions forming both the $N_2^+$ peak and that corresponding to the sum of the doubly ionized molecules from $e + N_2 \rightarrow N_2^{++} + 3e$ and the dissociated ions from $e + N_2 \rightarrow N + N^+ + 2e$. These three cross sections are listed as $Q(N_2^+)$, $Q(N_2^{++})$, and $Q(N_{2\,diss}^+)$, respectively in Fig. 16. In contrast to the atomic case, there is an inconsistency between the earlier and later data for $Q(N_2^+)$. The fact that the later data are much more scattered and consistently lower than the earlier data is as yet unexplained. There seems to be reasonable agreement between the results obtained by the two methods in the later data (the subtraction method data are shown as open circles, and the slope

data by solid circles in the figure), which makes this discrepancy somewhat puzzling. It may be cleared up in forthcoming measurements.

Separation of ions with the same charge/momentum ratio is impossible in our apparatus; thus, $N_2^{++}$ and $N^+$ ions will be focused into the ion collector at the same magnetic field. However, in mass spectrographic studies,[7] the appearance potentials (AP) for the production of both ions from electron impact on $N_2$ has been studied. For $N^+$, $AP(N^+) \approx 24.3$ ev while for $N_2^{++}$, $AP(N_2^{++}) \approx 49.5$ ev. This separation of 25 ev in appearance potential is sufficient to permit an unambiguous investigation of the dissociative ionization cross section below 49.5 ev.

From Fig. 15, it is seen that if direct, dissociative ionization occurs below 49.5 ev, its cross section is significantly less than $10^{-17}$ cm$^2$. Further improvement in the data collection techniques are required (and contemplated) to improve the sensitivity of the apparatus and to observe a better upper limit for $Q(N^+)$.

It must be concluded that below 50 ev the appearance of $N^+$ in mass spectroscopic studies is the result of a chain of reactions and that there is a very low probability that $N^+$ is formed directly. This is to be expected by application of the Frank-Condon principle and symmetry conservation rules to electron collisions with ground state $N_2$ molecules. The ratio of $N_2^{++}$ to $N^+$ formed by direct collision at energies above 50 ev may be very large and should be measured as soon as techniques are available to do so.

## C. ARGON

The argon data, shown in Fig. 17, were taken in order to compare measurements made using our apparatus with those obtained previously by another method. Bleakney[9] measured the *relative* efficiency for the production of $Ar^+$, $Ar^{++}$, $Ar^{+++}$, and $Ar^{++++}$ by electron impact on Ar and deduced the cross sections for each process by using the total ionization cross section measured by Smith[10] in a static gas.

Our measurements again yield cross sections that are lower than those obtained in a static gas, but the difference is very small for $Ar^+$ in the energy region above 200 ev. The discrepancy at electron energies below 100 ev is still larger than the statistical error; as yet we have been unable to account for a systematic error in this region. We suspect

that our data may be low above 250 ev (as much as 20% at 500 ev) due to a peculiarity of fringe electrical fields in the electron gun. These fields were capable of reducing the direct ion beam (deflectors off) measured at the neutral detector by about 30% when $V_e$ = 500 volts in the gun, but the effect should have been less for the ion signals because of the larger solid angle subtended by the ion collector. The gun has recently been modified to elimina · this source of error, and the possibility of a systematic error in these preliminary results will be examined.

The $Ar^{++}$ cross section is substantially lower than Bleakney's at all electron energies and the relative size of this cross section compared with that of $Ar^{+}$ is inconsistent with the results of Bleakney. As yet, we have no convincing explanation for this disagreement. A discussion of the possible causes of error will be given below.

## D. ERRORS AND UNCERTAINTIES IN THE RESULTS

### 1. Effects of Uncertainties in the Dimensions and Density Distributions of the Electron and Atom Beams

In computing the cross sections from Eq. (1) we assumed that both beam densities were uniform and the beams intersected each other exactly in an interaction volume of dimensions $L \times H \times S$. Figure 14 shows the interaction of the two beams in the ideal case where they intersect exactly in the vertical direction, each beam having a height $H$. Actually, the beams may have some overlap, or may not intersect completely. Even if the actual intersection geometry is not known, we can be satisfied that the upper and lower surfaces of each beam are parallel, that the electrons are very well directed in the direction $S$ (parallel to the magnetic field), and that the ions similarly travel parallel to $L$. The electron trajectories are considered below. For a detailed calculation of the cross section, we consider the production of ions from a thin slab of area $SL$ and height $\Delta h$. The upper and lower surface dimensions $S$ and $L$ are determined by the *actual* boundaries of the beams. The ion current $(di^+/dh)\Delta h$ produced in this volume element for a cross section $Q$ will be

$$\frac{di^+}{dh}\,\Delta h = \left(\frac{q}{e}\right) QSL\rho_a(h) j_e(h)\Delta h$$

where $j_e(h)$ is the average electron current density at height $h$, and $\rho_a(h)$ is the average atom beam density at height $h$.

The total ion current produced will be

$$i^+ = \left(\frac{q}{e}\right) QSL \int_{-\infty}^{\infty} \rho_a(h) j_e(h) dh \quad . \tag{7}$$

Note that if either $\rho_a(h)$ = constant = $\bar{\rho}_a$, or $j_e(h)$ = constant = $\bar{j}_e$, then we have

$$i^+ = \left(\frac{q}{e}\right) QSLH \bar{\rho}_a \bar{j}_e \tag{8}$$

which is equivalent to Eq. (1). If neither beam is uniform, the cross sections should be computed on the basis of Eq. (7).

In the actual measurements, we measured the total neutral beam current

$$i_a = KS \int_{-\infty}^{\infty} \rho_a(h) dh$$

(where $K$ is the necessary conversion coefficient), and then we computed a cross section from Eq. (8), using an apparent average beam volume-density

$$\langle \rho_a \rangle = \frac{i_a}{KSH} \quad .$$

This approximate value of the average is really

$$\langle \rho_a \rangle = \frac{1}{H} \int_{-\infty}^{\infty} \rho_a(h) dh \quad .$$

Similarly, we measured the total electron current

$$i_e = L \int_{-\infty}^{\infty} j_e(h) dh$$

and used the value

$$\langle j_e \rangle = \frac{i_e}{LH} = \frac{1}{H} \int_{-\infty}^{\infty} j_e(h) dh$$

in place of $j_e$ in Eq. (8).

Thus we computed an approximate cross section $\langle Q \rangle$ from the relation

$$i^+ = \left(\frac{q}{e}\right)\langle Q \rangle \, SLH \, \langle \rho_a \rangle \, \langle j_e \rangle$$

$$= \left(\frac{q}{e}\right)\langle Q \rangle \, SLH \cdot \frac{1}{H}\int_{-\infty}^{\infty} \rho_a(h)\,dh \cdot \frac{1}{H}\int_{-\infty}^{\infty} j_e(h)\,dh$$

$$i^+ = \left(\frac{q}{e}\right)\langle Q \rangle \, \frac{SL}{H}\int_{-\infty}^{\infty} \rho_a(h)\,dh \int_{-\infty}^{\infty} j_e(h)\,dh \quad . \tag{9}$$

To relate the computed value $\langle Q \rangle$ to the actual value $Q$, eliminate $i^+$ from (7) and (9), and obtain, after simplifying,

$$Q = \langle Q \rangle \frac{\int_{-\infty}^{\infty} \rho_a(h)\,dh \int_{-\infty}^{\infty} j_e(h)\,dh}{H\int_{-\infty}^{\infty} \rho_a(h) j_e(h)\,dh} \quad . \tag{10}$$

No error is incurred via uncertainties in $S$ and $L$, but only in assuming a uniform density in the vertical direction and also that the beams intersect exactly over the vertical distance $H$.

To determine the actual beam density profiles, the simple probe shown schematically in Fig. 14 was inserted into the drift space of the electron gun. The probe intercepted both beams just before they entered the interaction volume and permitted sampling of height $\Delta h = 0.020$ inch and the full width of each beam. Thus partial currents $\Delta i_e = j_e(h)L\Delta h$ and $\Delta i_a = K\rho_a(h)S\Delta h$ were measured, yielding sufficiently accurate values of $\rho_a$ and $j_e$ for our purposes. Typical density profiles of the electron beam and an ion beam are shown in Fig. 18. The error made in using $\langle Q \rangle$ as an approximation to $Q$ was determined to be a little over 1% for the profiles in Fig. 18, which were typical. Even though we approximated $\rho_a$ by using the ion beam, it is very unlikely that the atom beam density profile could be so dissimilar to the parent ion beam profile that an error significantly greater than 1% could arise. This small correction to $\langle Q \rangle$, an *increase* of 1%, was applied in calculating $Q$, but it is substantially less than the uncertainties due to noise and other effects.

## 2. Uncertainties in the Electron Energy (Interaction Energy)

Because of the great differences in the masses of the atoms and electrons, the atoms can be considered at rest with respect to the electrons; the energy of the electrons in the center of mass system was essentially the same as their laboratory kinetic energy for all energies considered. Hence only the electron energies need be considered in determining the interaction energy.

There are only two obvious sources of energy spread among the electrons and these do not include the thermal spread which they acquire upon emission from the indirectly heated cathode. The sources are space charge and drift grid bias.

The space charge in the electron beam will lower the mean kinetic energy; since the space charge potential is not uniform throughout the drift space, it will result in an energy spread among the electrons. An upper limit to the space charge effect was estimated by computing the potential depression in a beam of infinite cross section flowing between two plane grids: This will exceed the depression in a beam of finite dimensions. For a beam of infinite cross section, current density $j$, and maximum energy $eV_0$ flowing between two plane grids at potential $V_0$ and separated by a distance $S$, the minimum potential in the beam $V_{min}$ satisfies the relation

$$\frac{jS^2}{V_0^{3/2}} = \left[1 + 2\left(\frac{V_{min}}{V_0}\right)^{1/2}\right]^2 \left[1 - \left(\frac{V_{min}}{V_0}\right)^{1/2}\right] \text{(MKS units)} \quad .$$

We operated under conditions such that this calculated space charge depression did not exceed one volt near threshold and about 1 percent of the beam energy above 100 ev.

Space charge effects are easy to observe when the cross section is a steep function of impact energy, since the signal *vs* $i_e$ curve becomes nonlinear at high electron beam currents $i_e$. Therefore the linear portion at low $i_e$ was used to obtain the slope which was proportional to $i^+/i_e$. Space charge effects were eliminated using this procedure.

The second influence on the electron energy distribution was due to the 2.5 v bias across the drift space of the gun. It gave a linear increase of kinetic energy to the electron beam as it crossed the interaction

volume, and thus introduced a total spread in interaction energy of 2.5 ev. The mean electron energy was taken to be equal to $e(V_2 + 1.25)$ ev where $V_2$ was the voltage difference between the cathode and the first drift grid $G_2$.

## 3. Uncertainties and Errors in the Current Measurement

The magnitude of the computed cross section depends on the measurement of the currents $i_e$ of the electron beam, $i_a$ of the neutral beam, and $i^+$ of the product ions. The problem of determining the current in each of these beams consists of two parts, namely (1) the complete collection of the beam in question, with no contamination, and (2) the measurement of the current that is collected.

### a. Electron Beam

The average electron beam current $i_e/2$ is read directly on a dc meter which measures the current flowing to the second drift grid $G_3$ (see Fig. 4) and the collector A. The collection efficiency should be 100 percent. Secondary electron emission is apparently negligible under operating conditions. The electrical fields in the gun (due to the bias voltages) suppress secondary emission, and there is no change in currents with changes in these voltages about the operating values. A separate meter measures the current to the collector alone, which is about 95 percent of the current crossing the drift space; thus the second drift grid intercepts about 5 percent of the current. It is conceivable that the weak field placed across the drift space does not completely suppress secondaries, but this would only create an error in the 5 percent fraction of the current collected by $G_3$. (We have not yet thoroughly investigated the problem of secondary emission at energies above 250 ev, but there was certainly no evidence of difficulty from this effect at the lower energies.) The meters have been calibrated over the entire range of currents used, and the indicated current values are corrected during the runs according to data. The electron current measurements should be accurate to about 3 percent.

### b. Neutral Beam

In contrast to the above case, the measurement of the neutral beam is more susceptible to error. The collection efficiency is probably

nearly 100 percent since the nickel film which stops the beam can accept a circular beam 2.2 cm in diameter. The film has been examined each time the interaction chamber was opened up, and while there is some indication that fast particles have been stopped over most of this area, there is a marked discoloration in the center of about 8 × 10 mm which has the rectangular shape and size of the beam-limiting aperture in front of the electron gun. Thus the bulk of the beam struck the center of the collector and was considerably smaller than the collector dimensions.

The main source of error in measuring the neutral beam intensity lies in the fact that the thermocouple output is dependent upon the atom beam density distribution. The thermal junction is a small spot located in the center of a thin film of low thermal conductivity; hence the temperature at the junction will be greatest when the beam is centered on the film. A study of this effect was made using an ion beam. We measured the detector output voltage $V_t$ and the ion current $i_a^+$ for several values of the mass-analyzing magnet current which was varied to sweep the ion beam across the apertures of the interaction chamber. The ratio $V_t/i_a^+$ actually remained very constant over a fairly broad central portion of the current peak, and changed by only about 20 percent as $i_a^+$ dropped off to 50 percent of the peak value. No attempt was made to make the beam density uniform when the tests were made, but in view of the results, it is likely that the beam was fairly uniform. Sensitivity calibrations are usually reproducible to within 5 percent, but we have, at times, measured sensitivities which varied as much as 30 percent, and it would appear that these fluctuations were due to sharp structure in the beam density distribution, probably resulting from a peculiarity in the focusing conditions. We computed all cross sections using the same number for the detector sensitivity, $3.76 \times 10^{-2}$ volts/watt, and let any variations in the actual sensitivity appear as fluctuations in the cross sections. It is not known whether there is a consistent difference between the atom and ion beam density distribution, and thus the detector sensitivity, which would lead to a systematic error in the cross sections. However, we feel that such an error would be less than 10 percent, and would probably make the cross sections appear to be lower than the actual value, although this conclusion is moot. Total errors due to neutral detector uncertainties are probably less than 20 percent in these data.

The reliability of the detector is now being improved by gold-plating the central area of the film to increase (by an order of magnitude) the thermal conductivity over that portion which is struck by the beam. This modification should increase the accuracy of the detector to about 5 percent or better.

### c. PRODUCT ION CURRENT

The sensitivity of the main amplifier and detector is measured before each run to an accuracy of about 1 percent, and the calculated value of the preamplifier gain is probably good to 2 percent, which is similarly the error placed on the value of the input resistor. The total sensitivity of the amplifier-detector is thus known to an accuracy of about 3 percent.

The efficiency with which the ions are collected is less easy to establish. The ion collector is mounted behind two identical electrodes which serve to control the emission of secondary particles from the ion collector, to trap slow particles approaching the collector from the rest of the interaction chamber, and to define the surface area of the collector which is "seen" by ions leaving the interaction volume. These electrodes are thin, flat plates with a rectangular aperture cut out of each, and are mounted so that the common axis through the center of the apertures coincides with the trajectory of an ion which leaves the center of the interaction volume and has the proper curvature in the magnetic field to reach the center of the collector. The magnet pole faces are shaped so that the main ("gap") field focuses the ions in one direction (perpendicular to the field) and the fringe field exerts a weak defocusing action in the other (parallel to the field) so that the image of the interaction volume is a thick line at the collector. The $1.3 \times 2.2$ cm dimensions of the apertures in front of the collector were selected on the basis of plots of approximate trajectories, and were considered to be large enough to collect all ions of the proper momentum that were created in the interaction volume. If the collector apertures are wider than necessary, the graph of the ion signal plotted against magnetic field will show a flat-topped peak for each ionic species produced in the interaction region. Our studies of these graphs indicated that the collector apertures were of a marginal width in the direction perpendicular to the magnetic field: Some of the peaks were flat-topped while others were not. Evidently scattering of the beam in the ambient

gas made the particle trajectories more divergent, as they entered the interaction volume, than had been anticipated. Such scattering could also render the other aperture dimension too small. In order to estimate the collection efficiency of this first collection geometry, a new collector was built with both aperture dimensions about 25 percent larger than those of the original and a series of runs on argon was begun as this report was being written. A few cross sections for the production of $Ar^+$ were taken one evening, and these were about 20-30 percent higher than similar ones taken earlier. The signal vs magnetic field curves definitely showed flat tops, but a study of the shapes of the peaks indicated that the original dimensions perpendicular to the field were not small enough to cause much of an error (an upper limit of perhaps 10 percent). It is possible that the other dimension was too small, but this cannot be checked except by inference from the relative size of the cross sections taken with the two collectors. We intend to explore this point further with the enlarged ion collector, but our present data are limited to that obtained in the few initial runs mentioned,

All evidence from tests supported the view that secondary electrons were suppressed completely. It is possible that secondary ions could reduce the measured current, but tests with a direct ion beam showed that such an error is less than 2 or 3 percent.

An additional uncertainty in the ion current determination was due to the noise content of the total ion current collected. The modulated product ion current was many times smaller than the steady-state ion current resulting from electron-loss collisions between the fast beam atoms and the ambient gas in the vicinity of the interaction region. This large current of perhaps $10^{-12}$ to $10^{-11}$ amp had a noise content which varied mainly with conditions in the source. If a great deal of arcing occurred across the extraction gap, the main ion beam was itself noisy; consequently the neutral beam and finally the background current at the collector exhibited a high noise content. This noise was manifested in a continuous motion of the recorder pen, fluctuating about the average value. The actual signal level was estimated by eye after letting the recorder run for several minutes at each datum point. The length of time required to take a reasonable average depended upon the signal-to-noise ratio and increased as the ionization cross section decreased. It was generally possible to estimate an average value to an accuracy which was

about 5 percent of the magnitude of the rms noise fluctuations. Not all of the data were taken this painstakingly, however, and the error bars on most of the cross-section curves represent an *estimated* statistical uncertainty which was due largely to the effects of noise. These estimated errors are probably larger than the true standard errors would be. In the case of the early data on $N^+$ and $N_2^+$, the error bars actually represent the standard errors on the mean values of the averaged data for each point.

### *d.* Effect of the Magnetic Field on Electron Trajectories

If an electron crossing the drift space has a momentum component $p_1$ perpendicular, and a component $p_0$ parallel to the magnetic field, it will follow a helical path of length $S'$ in the drift space and the path length across the drift space must be increased by the ratio $S'/S = [1 + (p_1/p_0)^2]^{1/2}$. We have considered this effect for our gun geometry and have concluded that it is negligible, even at low drift energies.

## 4. Summary of the Errors and Uncertainties

The major uncertainties in the results stem from the neutral detector, from the noise in the primary ion beam, and from the possibility of error in the estimation of the ion collection efficiency. We estimate the statistical uncertainties to be less than 20 percent. It is conceivable that correction of a systematic error will raise the present cross sections about 20 percent; however, any such correction must be based on the results of further tests.

## V DISCUSSION OF THE RESULTS

The cross sections obtained on this apparatus are presented here as computed directly from measured quantities and some assumptions about geometrical dimensions. In general the cross sections have a reasonable energy dependence when compared with theory, in the case of N, or to previously measured total cross sections for $N_2$ and Ar. The absolute magnitude of the cross sections obtained are, at worst, within about 40% of comparable cross sections deduced from other measurements. Our measured values are generally lower in value than those obtained in static gases by Tate and Smith,[7] and Bleakney.[9] In the region from about 150 to 400 ev the results are quite close in both, but our curves do not peak as sharply at their maximum values near 100 ev as do those of Tate, and of Bleakney, so that our values are considerably lower (by ~40%) in the range below 100 ev. Even though our present values may be subjected to a systematic increase by up to 20% as a result of a re-evaluation of the ion collection efficiency in these runs, it is likely that the discrepancy below 100 ev will remain. We are unable to explain it at the present time.

Our absolute cross sections for the double ionization of argon are considerably lower than those of Bleakney measured in a static gas, and in fact our ratio of $Q(Ar^{++})/Q(Ar^{+})$ is only about ¼ to ⅓ as large as Bleakney's. It is possible that the discrepancy will be removed when the cross sections are measured with greater accuracy, but such a large change does not seem very likely to occur.

The most surprising outcome of the measurements to date is the lack of any signal from dissociative ionization below the threshold for double ionization, above which the two processes are indistinguishable in our apparatus. This indicates that the dissociative ionization of $N_2$ by electron impact is highly unfavorable as a direct process for impact energies below 50 ev, a conclusion which has at least qualitative theoretical support.

This latter observation lends some support to the suggestion that secondary processes may be responsible for the high ionization cross sections observed at low energies by Tate and Smith.[7] Perhaps the

observed dissociative or multiple ionization probabilities observed in mass spectrometric studies are also perturbed by secondary processes. Further study is required to clarify this point.

Although there are certain exceptions, most of our results are not inconsistent with the presently available theoretical and experimental determinations of the cross sections. The explanation of these discrepancies, resulting from further investigation, may be of substantial value to workers in the field of electron impact interactions.

# VI CONCLUDING STATEMENT

During the course of this work, an apparatus has been developed to a state of usefulness in studies of electron-atom (molecule) interactions. The use of a beam of fast atoms as the target in a crossed-beam arrangement, represents a new approach to these investigations. There are still minor uncertainties in the measurements; however, the cross sections obtained for the electron-impact ionization of N, $N_2$, and Ar are interesting and encouraging and demonstrate the usefulness of the technique.

In the future the apparatus will be refined still more and will be used to explore those fields of experimental studies for which it is particularly adapted. We intend to investigate further the dissociative ionization process and hope to couple the present technique with spectrographic studies in order to achieve greater insight into the process. We also intend to study the further ionization of ions. Investigations of this class of reactions of the type $e + Ar^{+} \rightarrow Ar^{++} + 2e$ are virtually limited to techniques such as the present one using beams of fast ions. It is beyond the purpose of this report to list the future applications of the apparatus. It is sufficient to say that the apparatus has proven to be capable of performing difficult electron studies, and its existence will further broaden the area of low-energy particle interactions amenable to experimental investigations. The fast beam and thermal beam techniques fortunately have overlapping capabilities, but in general their use will be complementary.

## ACKNOWLEDGEMENTS

The authors wish to express their indebtedness and gratitude to Messrs John Briski, George Conklin, and Ralph Leon, and Drs. Otto Heinz and Donald Lorents, all of whom have made substantial contributions to the development of the apparatus and the success of the program.

## REFERENCES


1. Peterson, J. R., O. Heinz, and C. J. Cook, Annual Report, Research on Collision Processes of Electrons and Atoms, Contract Nonr-2588(00). July 31, 1959.

2. Cook, C. J. and J. R. Peterson, Bull. Am. Phys. Soc. 2, 40 (1948).

3. Bederson, B., H. Malamud, and J. Hammer, Bul. Am. Phys. Soc. Ser. II, 2, 172 (1957); R. L. F. Boyd and G. W. Green Proc. Phys. Soc. 71, 351 (1958); R. Brackmann, W. Fite, and R. Neynaber, Phys. Rev. 112, 1157 (1958); W. Fite and R. Brackmann, Phys. Rev. 112, 1141, 1151 (1958). A review of recent work is given by Fite, W. L., Proc. Atomic & Mole. Beams Conf., Univ. of Denver, Colo. 1960, p. 7.

4. Peterson, J. R., Annual Report, Research on Collision Processes of Electrons and Atoms, Contract Nonr-2588(00), Dec. 7, 1960.

5. Neynaber, R. H., General Dynamics/Convair, Private Communication.

6. Seaton, M. J., Phys. Rev. 113, 814 (1959).

7. Tate, J. T., and P. T. Smith, Phys. Rev. 39, 270 (1932).

8. Hagstrum, H. P., and J. T. Tate, Phys. Rev. 59, 351 (1941); Vaughan, A. L., Phys. Rev. 38, 1687 (1931).

9. Bleakney, W., Phys. Rev. 36, 1303 (1930).

10. Smith, P. T., Phys. Rev. 36, 1293 (1930).

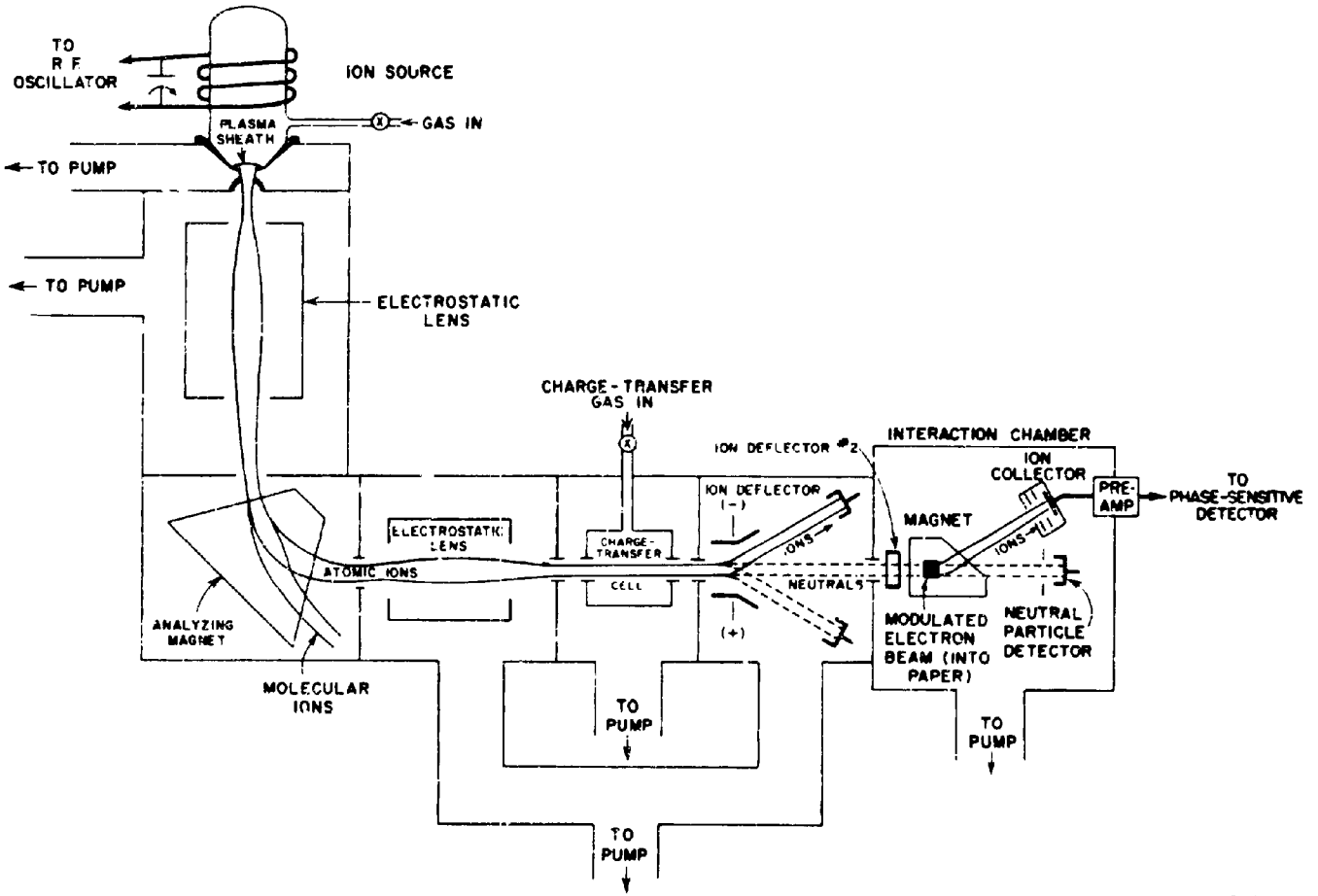


FIG. 1 SCHEMATIC DIAGRAM OF THE APPARATUS

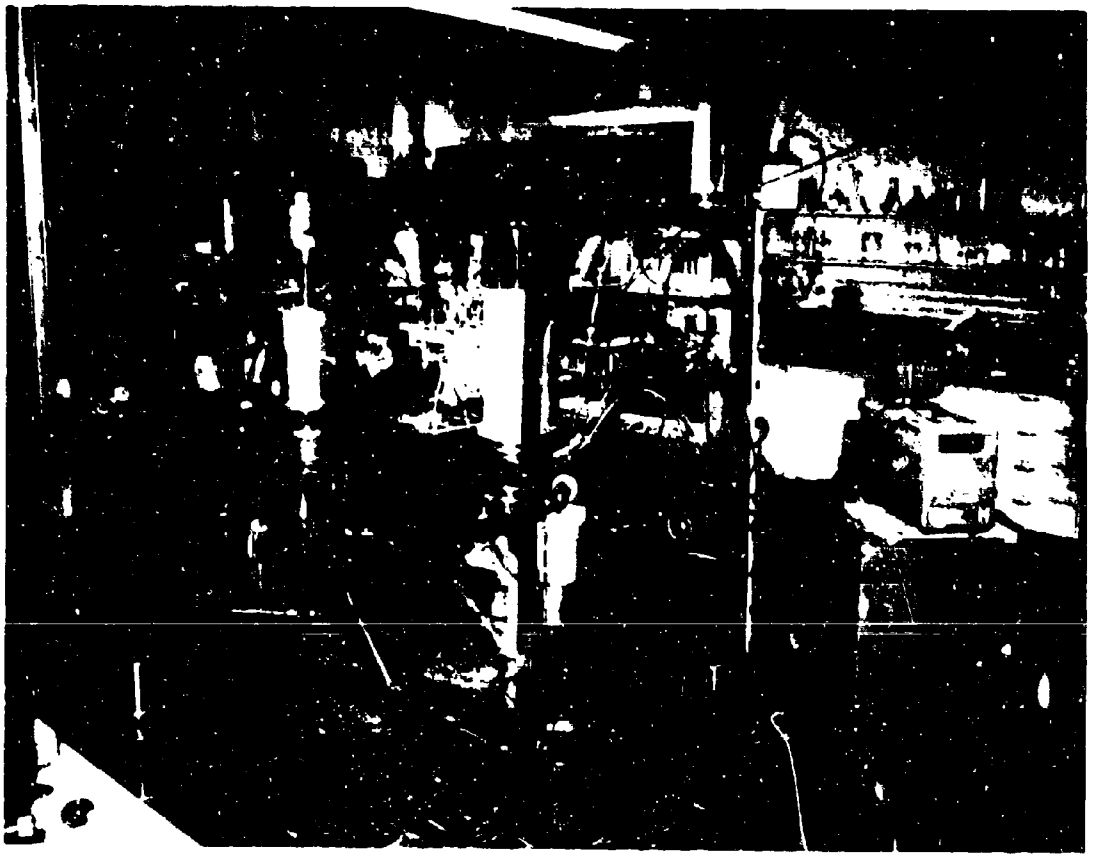

FIG. 2 EXPERIMENTAL APPARATUS

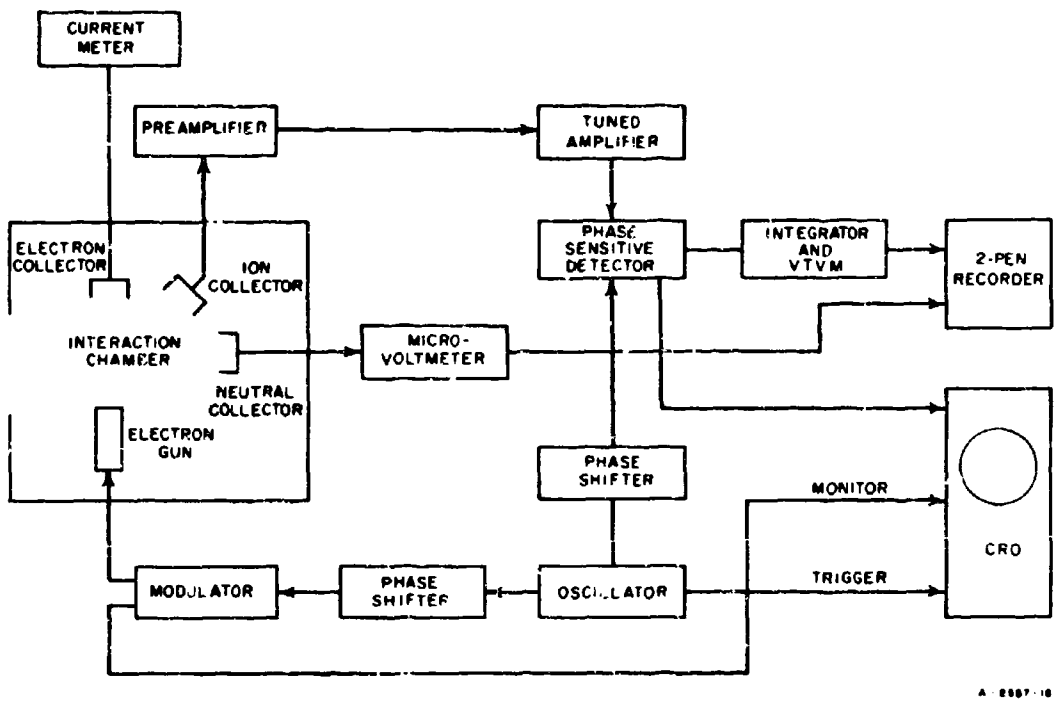


FIG. 3 BLOCK DIAGRAM OF THE DETECTION SCHEME

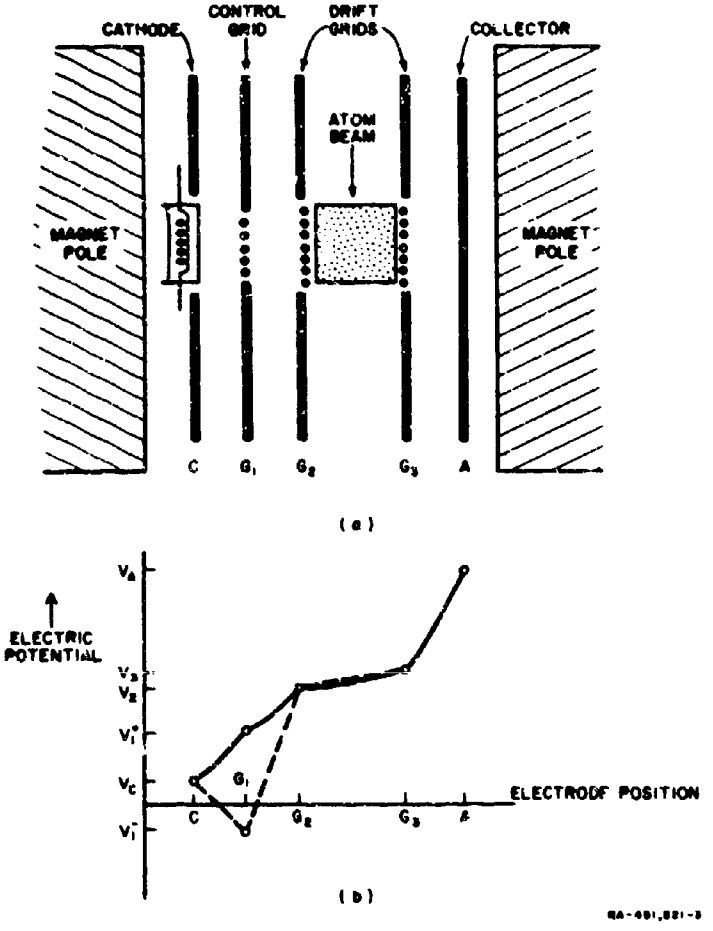


FIG. 4 ELECTRON GUN AND A DIAGRAM SHOWING TYPICAL RELATIVE OPERATING POTENTIALS ALONG THE BEAM AXIS

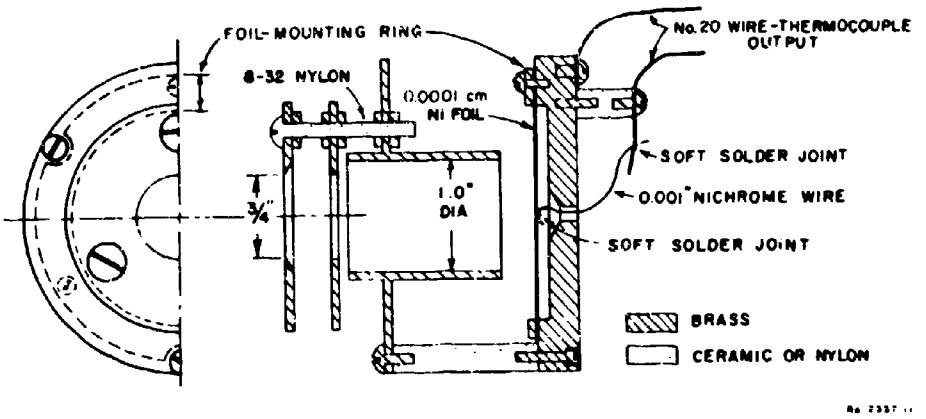


FIG. 5 NEUTRAL BEAM DETECTOR

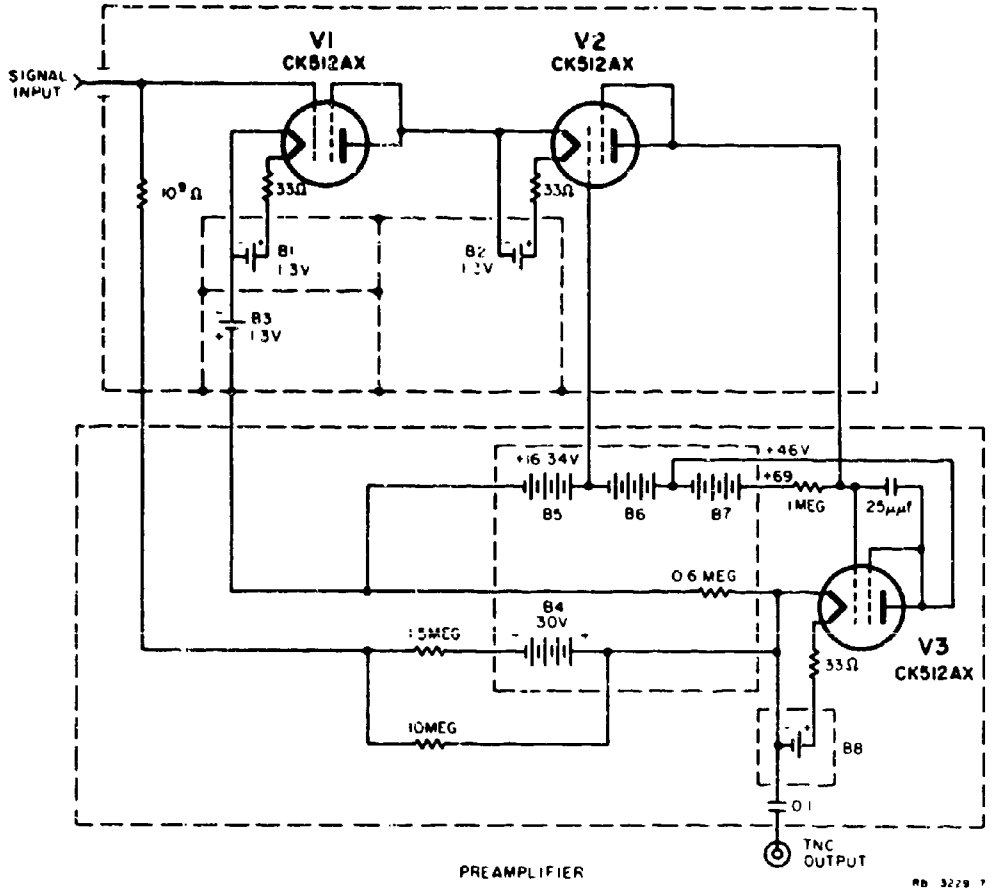


FIG. 6 PREAMPLIFIER CIRCUIT

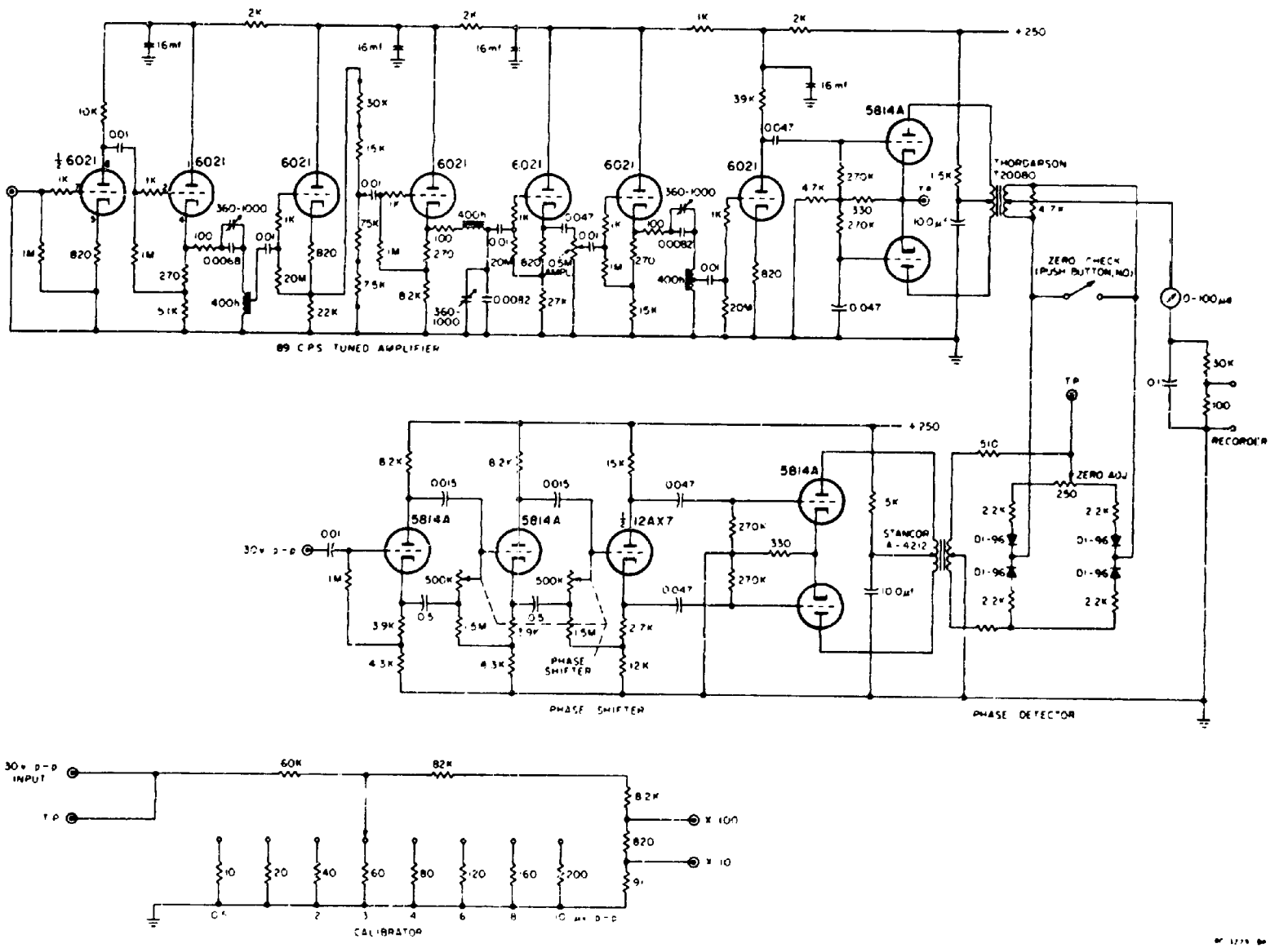


FIG. 7 AMPLIFIER AND DETECTOR

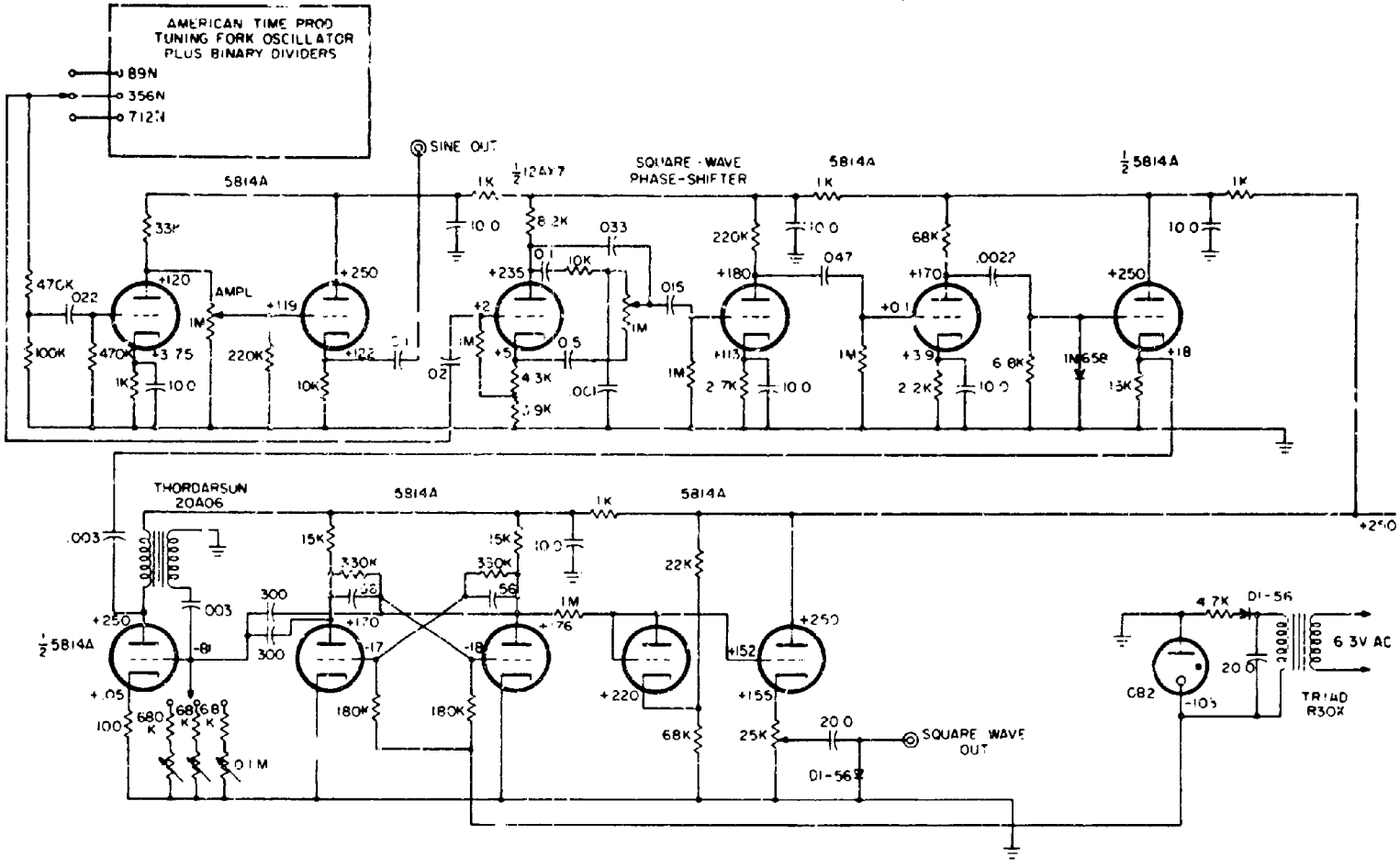


FIG. 8 OSCILLATOR AND MODULATOR

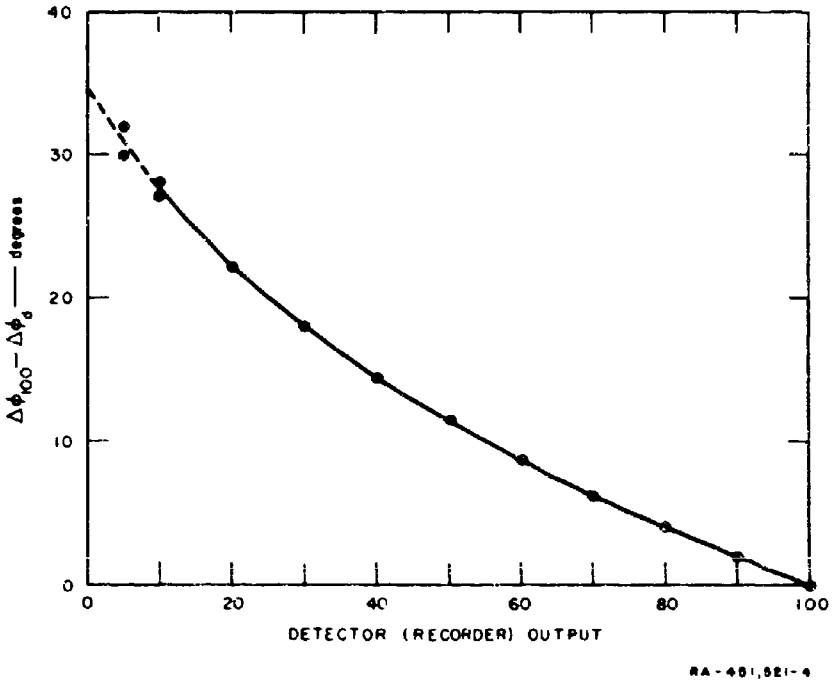


FIG. 9 VARIATION OF THE PHASE SHIFT THROUGH THE AMPLIFIER WITH SIGNAL OUTPUT LEVEL

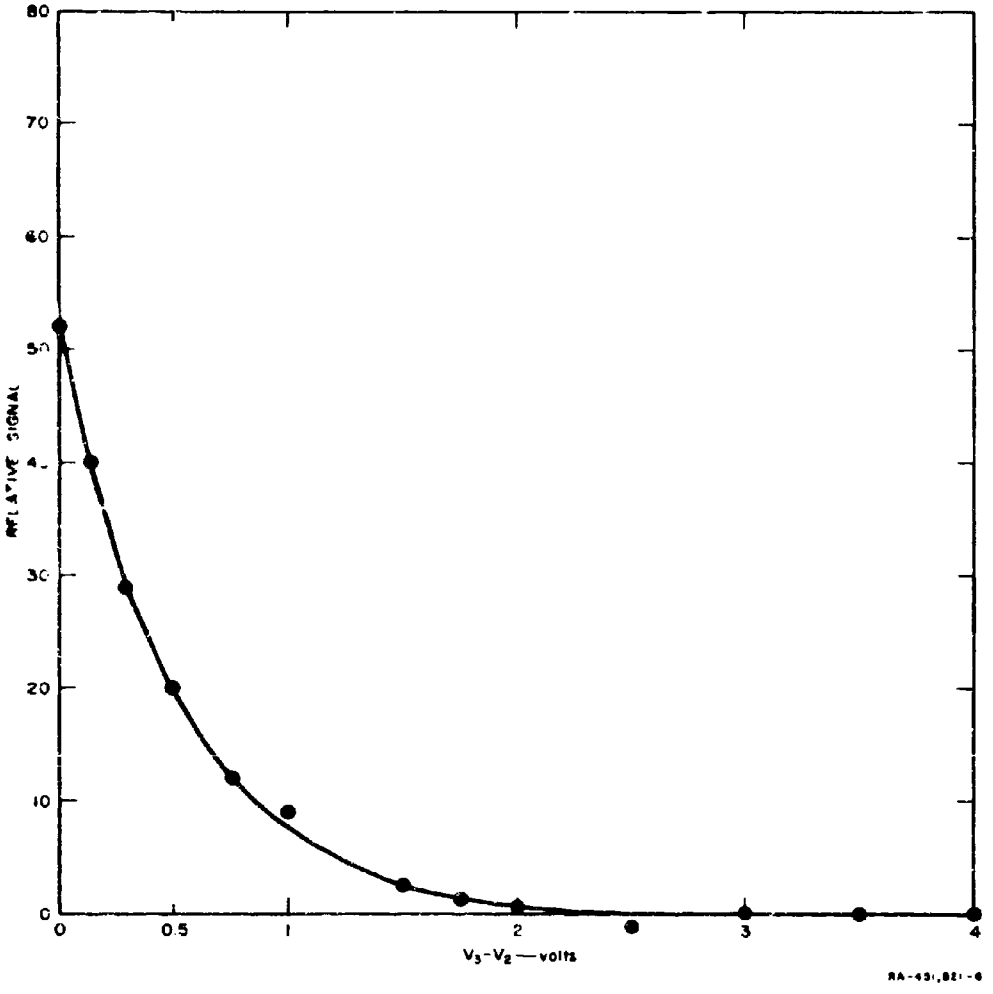


FIG. 10 SIGNAL DUE TO ELECTRON BEAM ONLY vs. BIAS VOLTAGE $V_3 - V_2$ ACROSS THE DRIFT GRIDS. $V_e$ = 70 ev, MAGNETIC FIELD = 1.5 kgauss, $V_A = V_2 + 5v$. THE SIGNAL IS UNCHANGED IN THE PLATEAU REGION IF $V_A = V_2$.

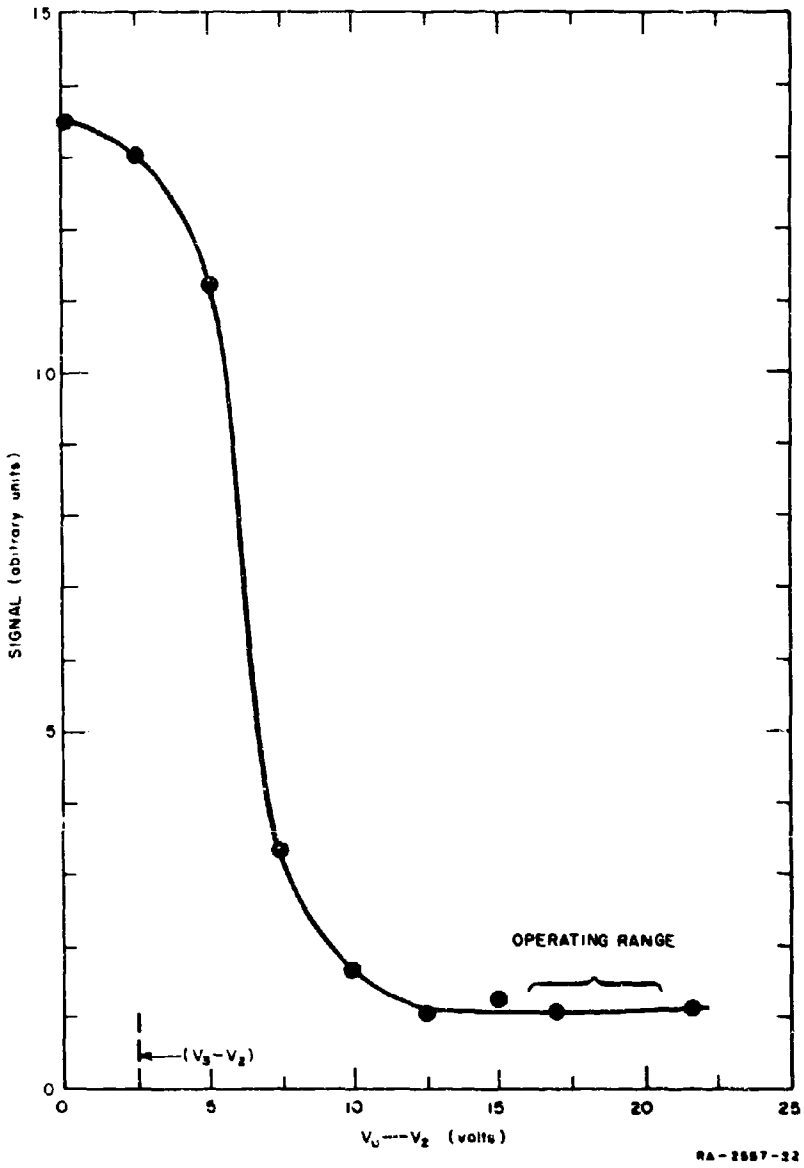


FIG. 11 SIGNAL vs. $V_A - V_2$ WITH THE ELECTRON AND ATOM BEAMS INTERSECTING AND THE MAGNET TUNED TO THE PEAK FOR THE $e + N \rightarrow N^+ + 2e$ SIGNAL. $V_3 = V_2 + 2.5v$.

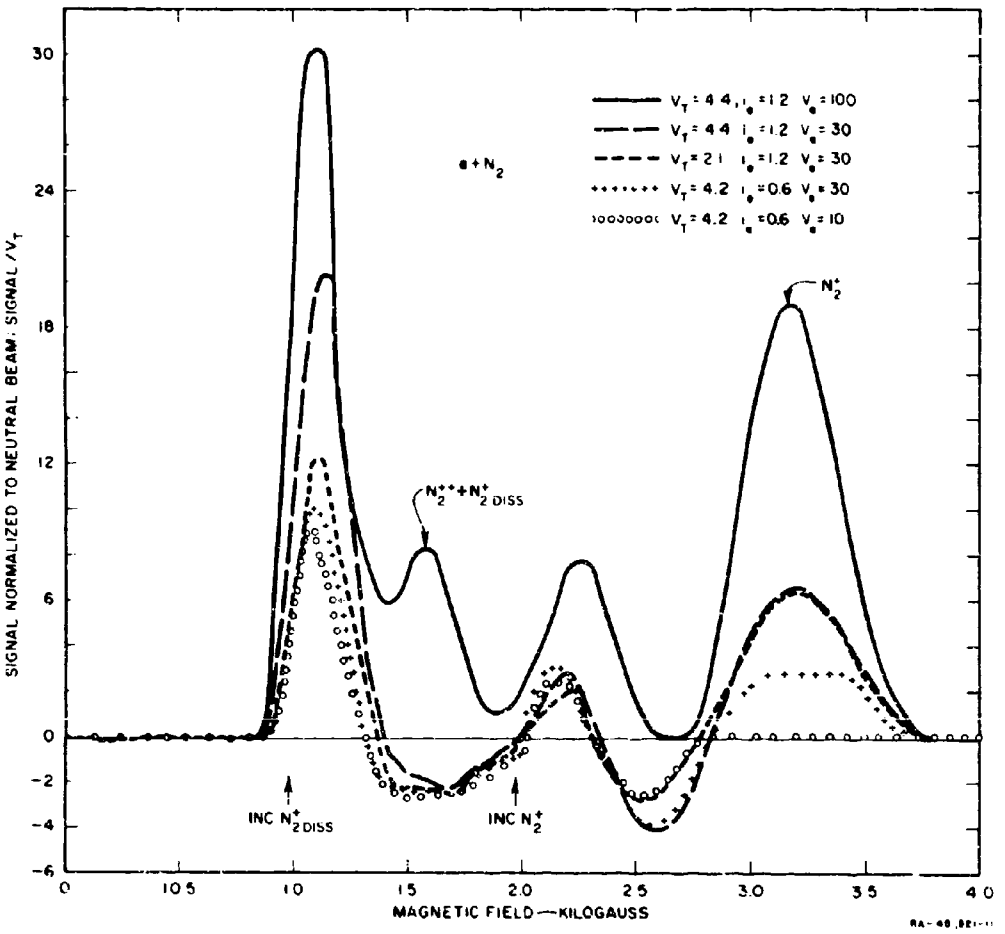


FIG. 12 e + $N_2$ SIGNAL vs. MAGNETIC FIELD, FOR SEVERAL ELECTRON ENERGIES ($V_e$) AND ATOM BEAM CURRENT DENSITIES ($V_t$)

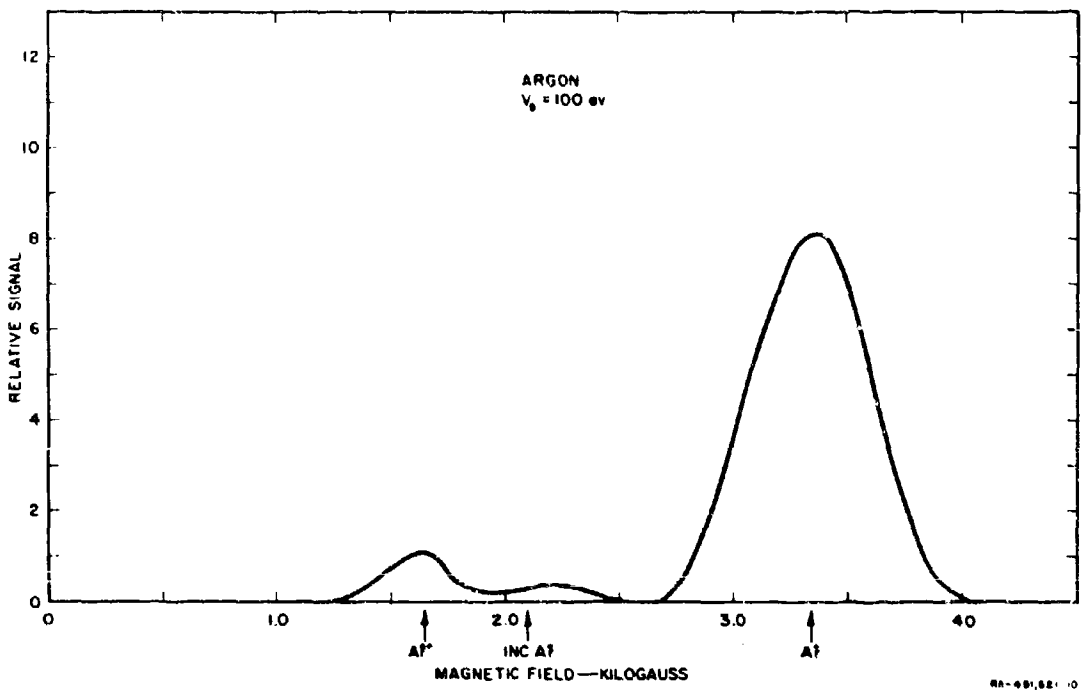


FIG. 13 e + Ar SIGNAL vs. MAGNETIC FIELD AT 100 ev ELECTRON ENERGY

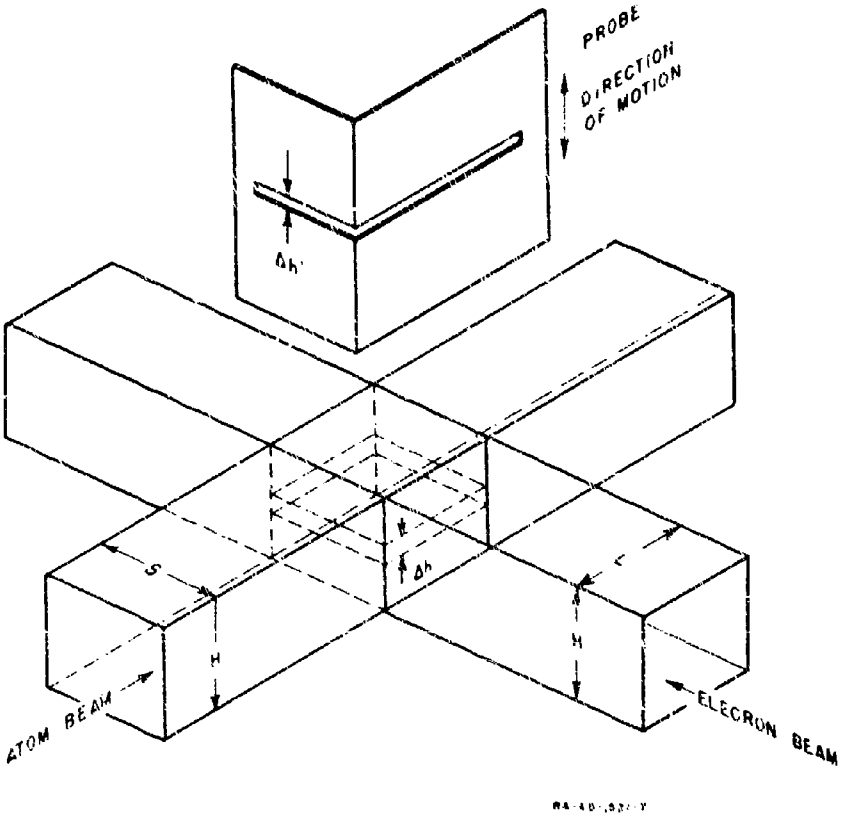


FIG. 14 DIAGRAM OF THE BEAM INTERACTION VOLUME, AND A SKETCH OF THE PROBE USED TO MEASURE THE BEAM DENSITY PROFILES

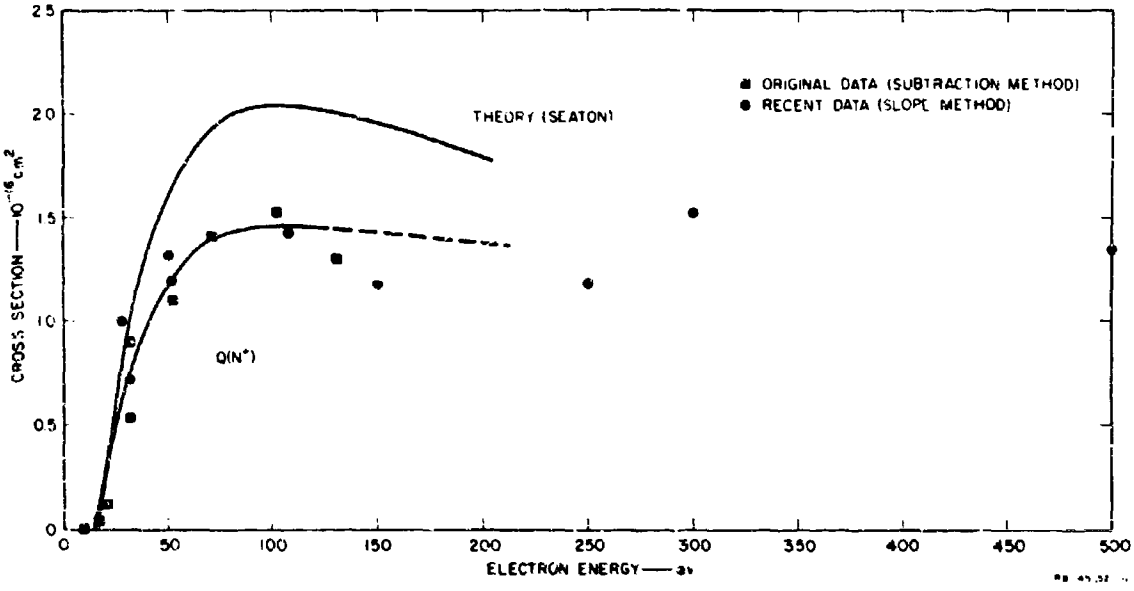


FIG. 15 CROSS SECTION FOR $e + N \rightarrow N^+ + 2e$

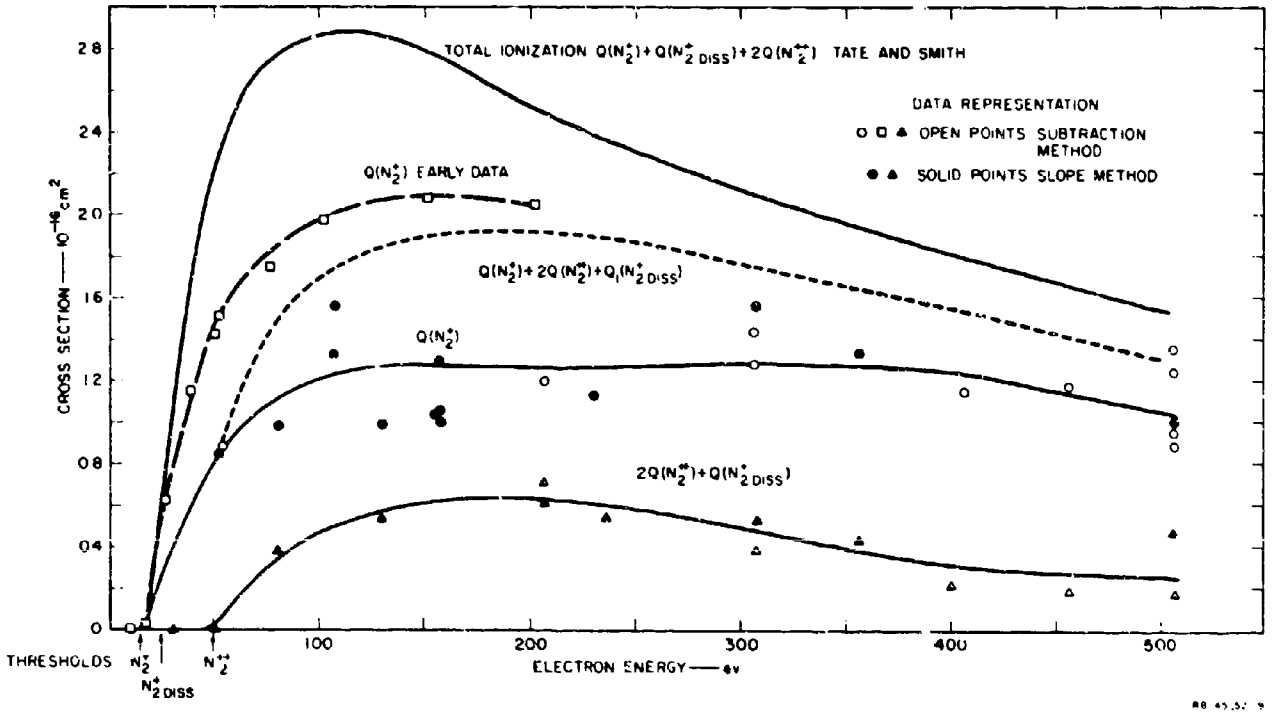


FIG. 16 CROSS SECTIONS FOR e + $N_2$ IONIZATION

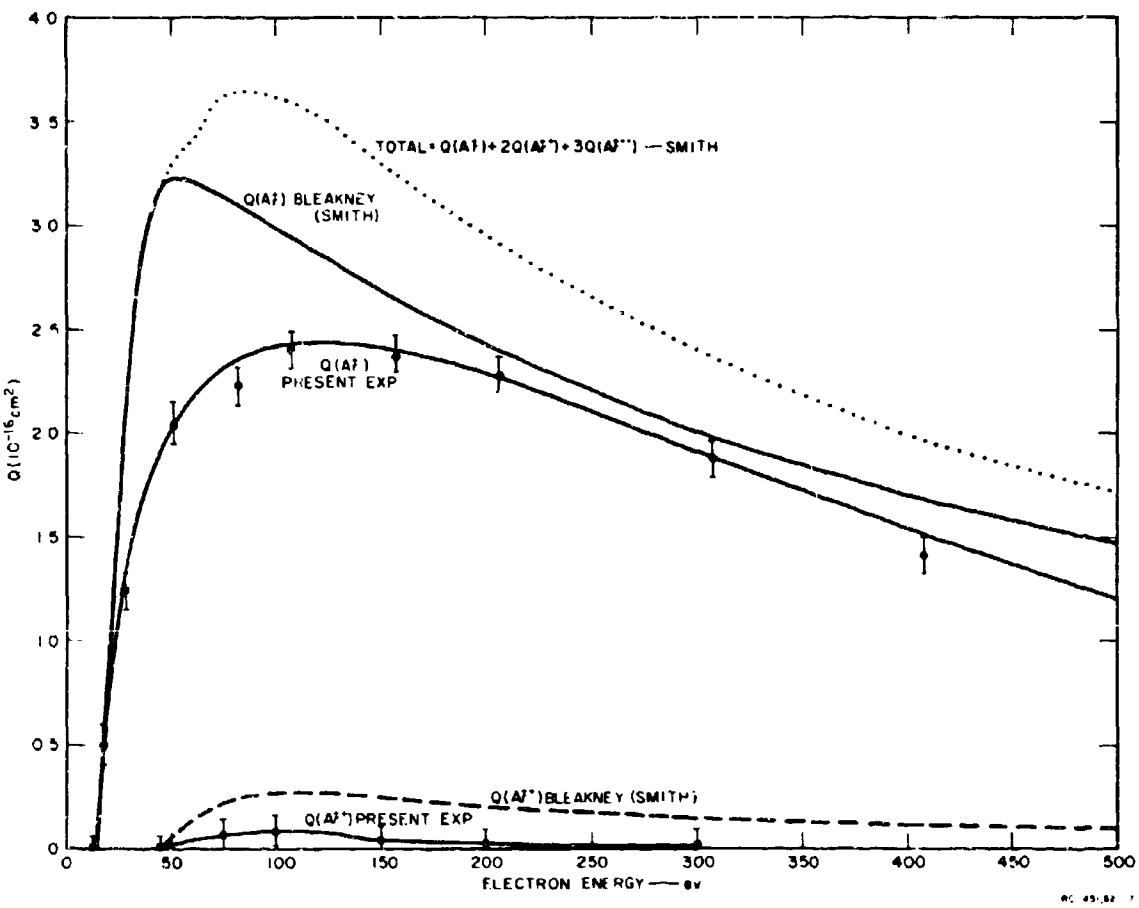


FIG. 17 CROSS SECTIONS FOR e + Ar IONIZATION

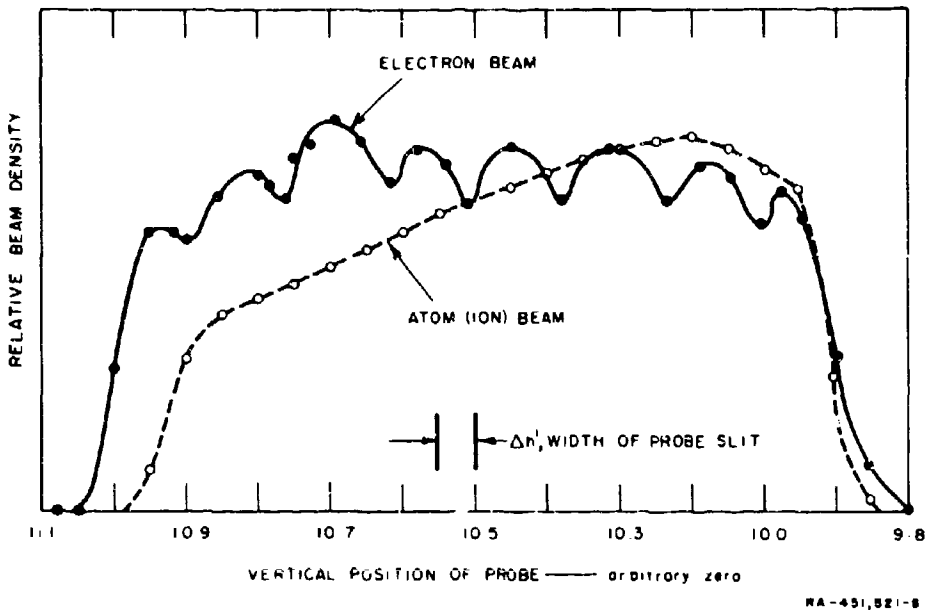


FIG. 18 DENSITY PROFILES OF THE ELECTRON AND ION BEAMS. THE DIPS IN THE ELECTRON BEAM PROFILE CORRESPOND TO THE SHADOWS OF THE GRID WIRES OF $G_1$, $G_2$, AND $G_3$